IEEE Access
Multidisciplinary ⋮ Rapid Review ⋮ Open Access Journal

Received 18 April 2023, accepted 14 May 2023, date of publication 16 May 2023, date of current version 1 August 2023.

Digital Object Identifier 10.1109/ACCESS.2023.3276860

RESEARCH ARTICLE

Review on Unidirectional Non-Isolated High Gain DC–DC Converters for EV Sustainable DC Fast Charging Applications

R. VENUGOPAL[1], BALAJI CHANDRASEKAR[1], (Member, IEEE), A. DOMINIC SAVIO[1], (Member, IEEE), R. NARAYANAMOORTHI[1], (Member, IEEE), KAREEM M. ABORAS[2], HOSSAM KOTB[2], YAZEED YASIN GHADI[3], MOKHTAR SHOURAN[4], AND ELMAZEG ELGAMLI[4]

[1]Department of Electrical and Electronics Engineering, SRM Institute of Science and Technology, Kattankulathur, Chennai 603203, India
[2]Department of Electrical Power and Machines, Faculty of Engineering, Alexandria University, Alexandria 21544, Egypt
[3]Department of Computer Science and Software Engineering, Al Ain University, Abu Dhabi, United Arab Emirates
[4]Wolfson Centre for Magnetics, School of Engineering, Cardiff University, CF24 3AA Cardiff, U.K.

Corresponding author: Elmazeg Elgamli (elgamlies@cardiff.ac.uk)

ABSTRACT Modern electrical transportation systems require eco-friendly refueling stations worldwide. This has attracted the interest of researchers toward a feasible optimal solution for electric vehicle (EV) charging stations. EV charging can be simply classified as Slow charging (domestic use), Fast charging and Ultrafast charging (commercial use). This study highlights recent advancements in commercial DC charging. The battery voltage varies widely from 36V to 900V according to the EVs. This study focuses on non-isolated unidirectional converters for off-board charging. Various standards and references for fast off-board charging have been proposed. Complete transportation is changed to EVs, which are charged by the grid supply obtained by burning natural fuels, contributing to environmental concerns. Sustainable charging from sustainable energy sources will make future EV completely eco-friendly transportation. The research gap in complete eco-friendly transit is located in interfacing sustainable energy sources and fast DC EV charging. The first step towards clean, eco-friendly transportation is identifying a suitable converter for bridging the research gap in this locality. A simple approach has been made to identify the suitable DC-DC converter for DC fast-charging EVs. This article carefully selected suitable topologies derived from Boost, SEPIC, Cuk, Luo, and Zeta converters for clean EV charging applications. A detailed study on the components count, voltage stress on the controlled and uncontrolled switches, voltage gain obtained, output voltage, power rating of the converters, switching frequency, efficiency obtained, and issues associated with the selected topologies are presented. The outcome of this study is presented as the research challenges or expectations of future converter topologies for charging.

INDEX TERMS DC fast charging, eco-friendly EV, highly efficient, high gain, sustainable charging.

I. INTRODUCTION

The emission from conventional oil burnt vehicles directly affects the air quality, affecting the ecosystem. 24% of CO2 emission is only due to the combustion of fossil fuels. The International Energy agency reports 37.0 Giga tons of CO2 emissions expected by 2035 [1].To control the continuous rise in global mean temperature, 196 countries signed the Paris Agreement in December 2015 [2]. As an alternative to conventional vehicles, electric vehicles are being pushed into the market to limit their dependence on oil for transportation and CO2 emissions. The inrush of EVs alone indirectly reduces pollution to some extent. Countries like India which generate electricity by burning coals that charge the EVs, will indirectly contribute to the emission of greenhouse gases [3].

The associate editor coordinating the review of this manuscript and approving it for publication was Kan Liu.

Environmental concerns of the conventional IC-based automotive sector enable high EV penetration into the market over the decade. Improved battery technology and reduced greenhouse gas emissions have led to drastic growth in the EV sector. Leading car manufacturers like Toyota and Volvo are planning to move entirely to hybrid/EVs [4], [5], [6]. Although EV are not new, the first commercial EV were in the late 1800s and the early 1900s. However, it is unattractive due to premature technology, shorter distance, and high cost [7]. The challenges lie with EV charging par with the traditional refueling stations, which takes less time. The major issues associated with EVs are price, cover range, and a lack of charging infrastructure [8], [9], [10].

Current EV charging is onboard, and the DC off-board charging station is the most common mode of charging. Onboard chargers have merits such as the choice of time and place for charging, availability of grid supply, better battery life, and low power level of charging [6], which causes onboard charging to charge for the entire night; hence, it is not a replacement for the conventional fueling method. The DC fast chargers were placed outside the vehicle. Hence, the power levels should be greater than 50 kW. The charging structures can be AC and DC grid-based [7], [11], [12], [13], [14]. The AC power distribution grid architecture has the advantage of a ripened distribution system with advanced protection technology. The DC grid architecture has numerous virtues par with the AC grid: ease of integration of renewable energy and storage equipment, low cost and smaller size, better efficiency, etc [15], [16], [17], [18].

Though the number of potential barriers lines up when considering large-scale renewable integration to the electrical systems, renewable energy, such as wind and solar supply variation has no relationship with the load variations [19], [20], [21]. The availability of renewable energy is a major concern, that is, solar energy depends on sunshine and wind energy depends on wind blowing. Therefore, there is a very good scope of research on power electronics in EV applications [22], [23], [24].

A previously published article commented on EV charging power converters with AC grids, standards, and fast charging with medium voltage grids. However, no article focuses on the off-board, AC, and DC fast-charging power electronics converter topologies. To address these research gaps, this review uncovers recent contributions with an exhaustive study of converters for EVs. The contributions of this review are as follows.

- A thorough examination of DC-DC converter topologies appropriate for EV applications.
- Topologies of DC-DC converters are classified based on voltage multiplier cells.
- Comparison of segregated topologies best suited for EV applications.
- Identify the demerits of converter topologies.
- Research gap in the domain and suggestions for identified EV charging.

EVs and EV rapid DC charging are discussed in Section II. Section III thoroughly categorizes the converter topologies in EV based on factors such as power flow direction, isolation, and conversion stages. Section IV describes the different Boost converter-derived or modified topologies. The several SEPIC converter topologies derived are discussed in Section V. Section VI explains the Cuk converter derived or modified topologies. The different derived and modified topologies of the Luo converter are discussed in Section VII. The Zeta converter-derived or modified topologies are addressed in Section VIII. The review view on the unsolved research challenges is explained in Section IX. In section X, the conclusions of this article. Fig. 1 displays the organization of the review article.

II. EVs AND DC FAST CHARGING

A. TYPES OF EVs

The three types of EVs are i. Battery electric vehicle (BEV) ii. Plug-in hybrid electric vehicles (PHEV) iii. Hybrid EV (HEV). BEVs can be easily charged at home by plugging them into an electrical supply. Tesla Model S, Nissan Leaf, BMW i3, ford focus EV, etc. are commercial BEVs. PHEV are suitable for long distances because they combine IC engines with electrical motors [25]. This PHEV can operate in the charge-depleting mode, that is, isolates the IC engine and drives the wheels through battery operation until the threshold SOC is reached. After reaching minimum SOC, it operates at charge-sustaining mode. BMW i8, and Cadillac ELR, are a few commonly available PHEVs. In a hybrid electric vehicle, the ICE and electric motor operate simultaneously. Here, the electric motor is powered only by regenerative braking and batteries, but there is no charging facility from the Utility Grid. AUDI Q5 hybrid, Acura ILX hybrid, and BMW active hybrid 3 are the few available HEVs. Over 16.5 million EVs were on the road in 2021, which tripled in three years [22], [26], [27]. EV sales in India over the last ten years represented in Table 1 were considered from [9], [28], and [29].

The sales of EV have grown gradually over the past ten years as indicated in Table 1 and the year 2022, the sales growth is 210% compared to the overall EV sales in the past. The two-wheeler and three-wheeler sales cover 62.25% and 33.74% respectively of the overall EV sales in the year 2022. Fig. 2 represents the Percentage Growth of EV over the decade and Fig. 3. Represents the various types of vehicle sales percentage in the year 2022 on total vehicle sales in 2022.

B. EV CHARGING

The charging stations can be classified as slow, fast, and ultra-fast charging based on voltage levels. The two most common charging ways are conductive and inductive charging. The conductive charging method is more widely used than inductive charging. On-board and off-board charging are the two types of conductive charging [30].

Level-1 charging is slow; it takes 10-12 hours to charge the EV battery. It connects to the EV port using a regular j1772 connection [31], [32], [33]. Though the cost was

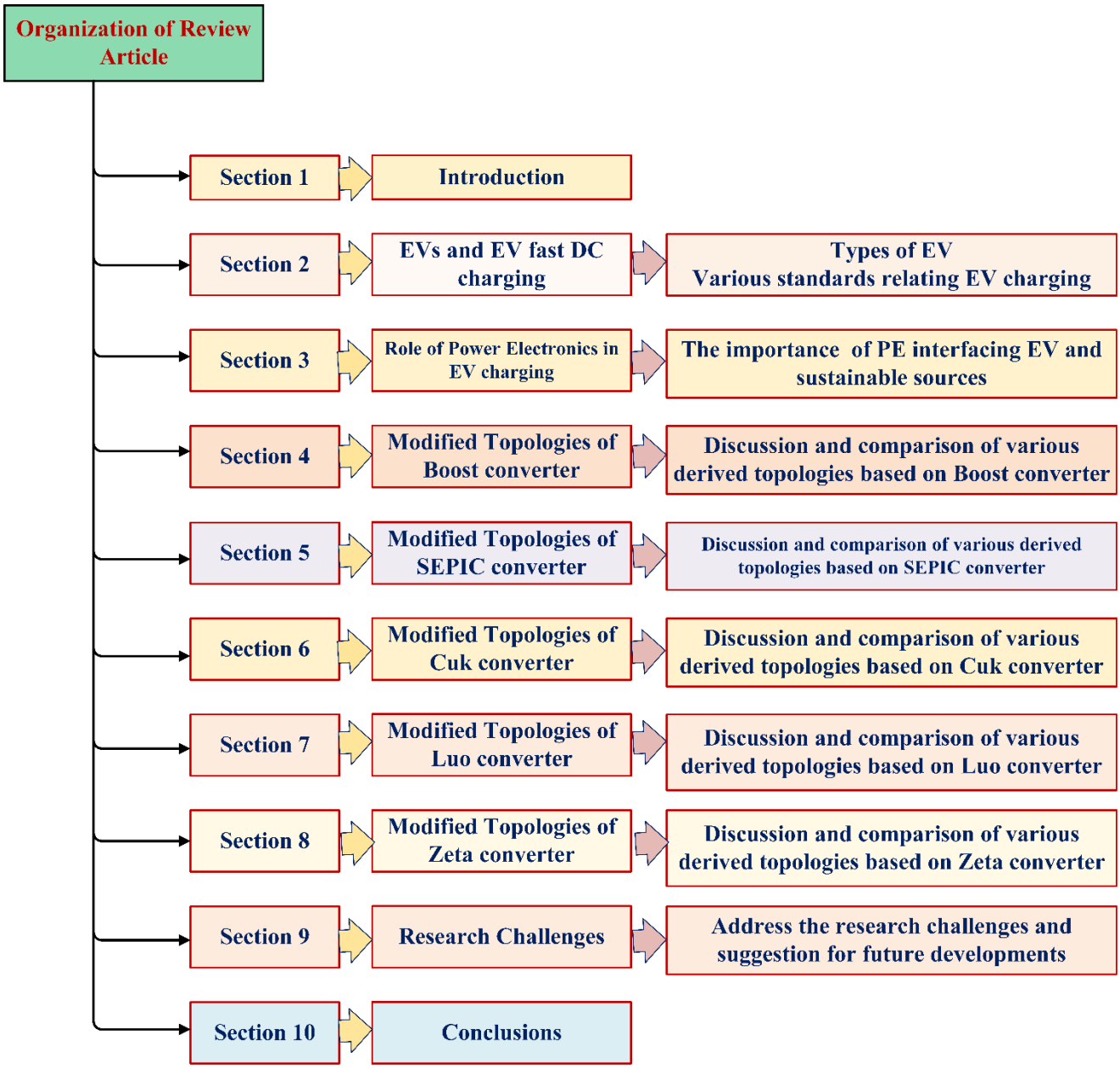

FIGURE 1. Review article organization.

comparatively low, the charging time was extended. This has led to the development of a level-2 charging station. Table 2 illustrates the level of EV charging in the DC & AC distribution grids. The charging time was reduced to 4-6 hours for full charging. Though the charging time is reduced considerably par with slow charging, compared to conventional fueling vehicles, charging time is still high [34], [35]. This results in the next level of charging, called fast DC charging. The output voltage for DC fast charging is 480 V DC or higher, and the charging duration is around 30 minutes. DC fast charging stations are significantly more expensive than level 1 and level 2 charging stations [31], [36], [37]. The ideal capacity for DC fast charging is 50 kW and has recently been upgraded to 350 kW for off-board charging. When compared to the time necessary to recharge a traditional fuel vehicle, the demand for ultra-quick/extremely rapid charging is need of hour. The technical aspects of state-of-the-art DC fast charging are presented in Table 3.

The power rating of various EV model chargers ranges from 50 kW to 350 kW, and the ampere rating ranges from 120A to 375A. Table 4 presents various ratings of off-board DC fast charging [35].

In the world, China and Europe held major EV charging networks, which share 48% in China and 33% in Europe

TABLE 1. The progress of EVs in india in over 10 years, data from vahan.

Year	2 Wheelers	3 Wheelers	4 Wheelers	Buses	Goods Carriers	Total	% Growth
2013	1989	36	374	1	43	2443	
2014	1678	12	481	3	20	2194	-10.1924
2015	1454	5399	678	3	19	7553	244.2571
2016	1459	46561	621	4	54	48699	544.7637
2017	1523	82238	820	17	533	85131	74.81057
2018	16572	108289	988	49	657	126555	48.65913
2019	29756	131375	847	468	53	162499	28.40188
2020	28632	88227	3179	88	13	120139	-26.0679
2021	153523	153679	12112	1177	1084	321575	167.6691
2022	622337	337335	37792	1932	453	999849	210.9225
% Sales (2022)	62.25%	33.74%	3.78%	0.2%	0.05%	100%	0.03%
Total	858923	953151	57892	3742	2929	1876637	1283.224
2013	1989	36	374	1	43	2443	

*sales in a number of units

TABLE 2. EV charging level in AC and DC distribution grids.

Level	Level 1			Level 2			Level 3		
Parameters	V	I	P	V	I	P	V	I	P
AC Grid	120-230	16	2	240-400	80	20	480-600	100	50
DC Grid	200-450	80	36	200-450	200	90	200-600	400	240

*V-Voltage (Volt); I-Current (A); P-Power (kW)

TABLE 3. State-of-the-art DC fast-charging technical aspects.

Model	Power (kW)	Input Voltage (V)	Output DC Voltage (V)	Current output (A)	Efficiency (%)	Weight (kg)	Time to charge 200 miles (minutes)
ABB Terra	50	480 (VAC)	200-500	120	94	400	72
Tritium VE30EFIL-RT	50	380-480 (VAC) 600-900 (VDC)	200-500	125	>92	165	72
PHIHONG Integrated Type	120	380-480 (VAC)	200-750	240	93.5	240	30
Tesla Super Charger	135	380-480 (VAC)	50-410	330	91	600	27
EVTEC Espresso & Charge	150	400 (VAC)	170-500	300	93	400	24
ABB Terra HP	350	400 (VAC)	150-920	375	95	1340	10

in 2021. In 2015, the Indian government recognized the National Institute of Transforming India (NITI) as encouraging eco-friendly products. Niti Aayog launched the Faster Adoption and Manufacture of EVs (FAME). To install 2900 charging stations in 25 states of India, the FAME II program provides a subsidiary of about 135 million USD. NHAI set a target to install an EV charging station for every 40–60 km covering 35000–40000 km of the National Highways by 2023 [1].

In comparison to other nations, China has already established 51 % of slow-charging stations and 82 % of fast-charging stations. Fast charging [7], [38], [39], wireless charging [40], [41], [42], [43], bidirectional charging, and medium-voltage charging [31], [33], [44], [45] have been reported. Only a single-phase supply is available in many locations off cities along highways. Upgrading the electrical infrastructure at all locations incurs high installation costs. New battery technologies have been proposed

TABLE 4. Ratings of off-board DC fast charging.

	Voltage Level (V)	Power Level (kW)	Characteristic range each minute of charge (km)	Time to charge to cover 200km (Minutes)
Fast charging	480	50	4.70	37
Tesla supercharge	480	140	13.15	13
Ultrafast charging	800	400	37.50	4.7

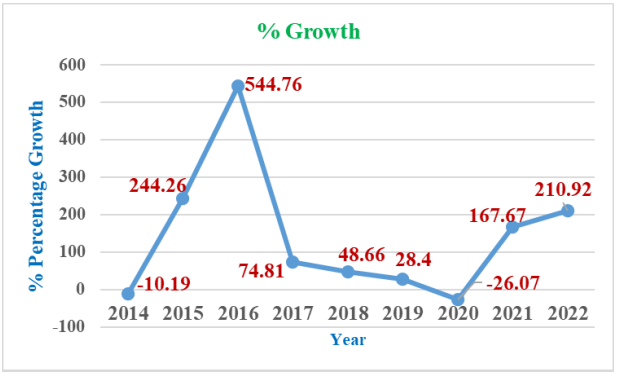

FIGURE 2. % Growth vs year.

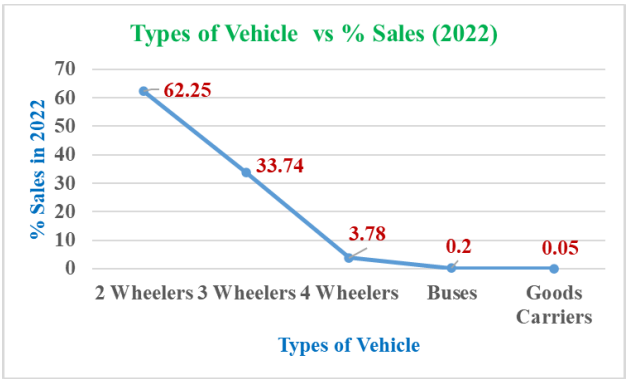

FIGURE 3. Sales percentage vs vehicle type (2022).

to cover a longer distance for a single charge. However, it costs 50-60 % of the total vehicle cost [21], [37], [46], [47].

III. ROLE OF POWER ELECTRONICS IN EV

Power electronic converters play a vital role as a bridge between the electrical power network and vehicle battery. Therefore, power electronic converters are expected to be highly reliable and cost-efficient [48], [49], [50]. Several converters like DC/AC and DC/DC with various ratings are involved in EV applications, as depicted [48], [51], [52], [53], [54], [55], [56].

Despite tremendous developments in EV technologies, a potential barrier still exists with EV battery charging (power

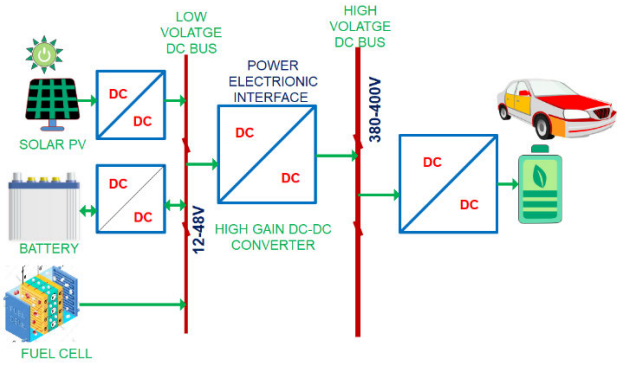

FIGURE 4. The architecture of sustainable EV charging.

electronics converter topologies) [57]. High-performing converters for battery charging play a significant role in future developments. Charger design challenges are mainly due to various battery voltages and power sources. The chargers must adopt various safety standards for EVs [58]. For example, UL 2202 ensures the protection of the charging system, and ECE R 100 ensures electric shock protection. Various converter topologies, such as isolated and non-isolated, unidirectional, and bidirectional, exist to meet the requirements of EV charging [8], [10], [56], [59].

Converters operating at high duty cycles (power switches operate for a long period, i.e., close to the switching period), invariably increase the voltage and current stress on the components. Consequently, converters suffer from conduction losses [32], [60]. The output diode will conduct opposite to the power switch (for a shorter duration), making the diode suffer from a reverse recovery problem. Isolated converters provide high gain by simply altering the transformer's turn ratio. However, due to the transformer's leakage inductance, this causes enormous voltage spikes across the switches, lowering overall efficiency. Many isolated and non-isolated converter topologies have been reported in the literature for high-gain applications [25], [50], [61], [62], [63].

To charge and discharge an EV's battery, or Energy Storing Elements (ESE), a bi - directional DC-DC converter is used to connect the ESE and loads on the EV [64]. However, unidirectional converters are also incorporated equally to supply the sub-systems of the EV, such as sliding windows, side mirror adjustments, wiper motors, music systems, and lighting. The architecture of a sustainable EV charger is illustrated in Fig.4. Various renewable energy resources are interfaced to the low-voltage DC bus, whose voltage rating is between 12V and to48V. The power electronic interface satisfies the EV charger's demand by converting low voltage to high voltage in the range 380-400V DC.

A. CLASSIFICATION OF UNIDIRECTIONAL CONVERTER

In general, DC-DC converters are categorized as isolated or non-isolated. Non-isolated converters are further classed

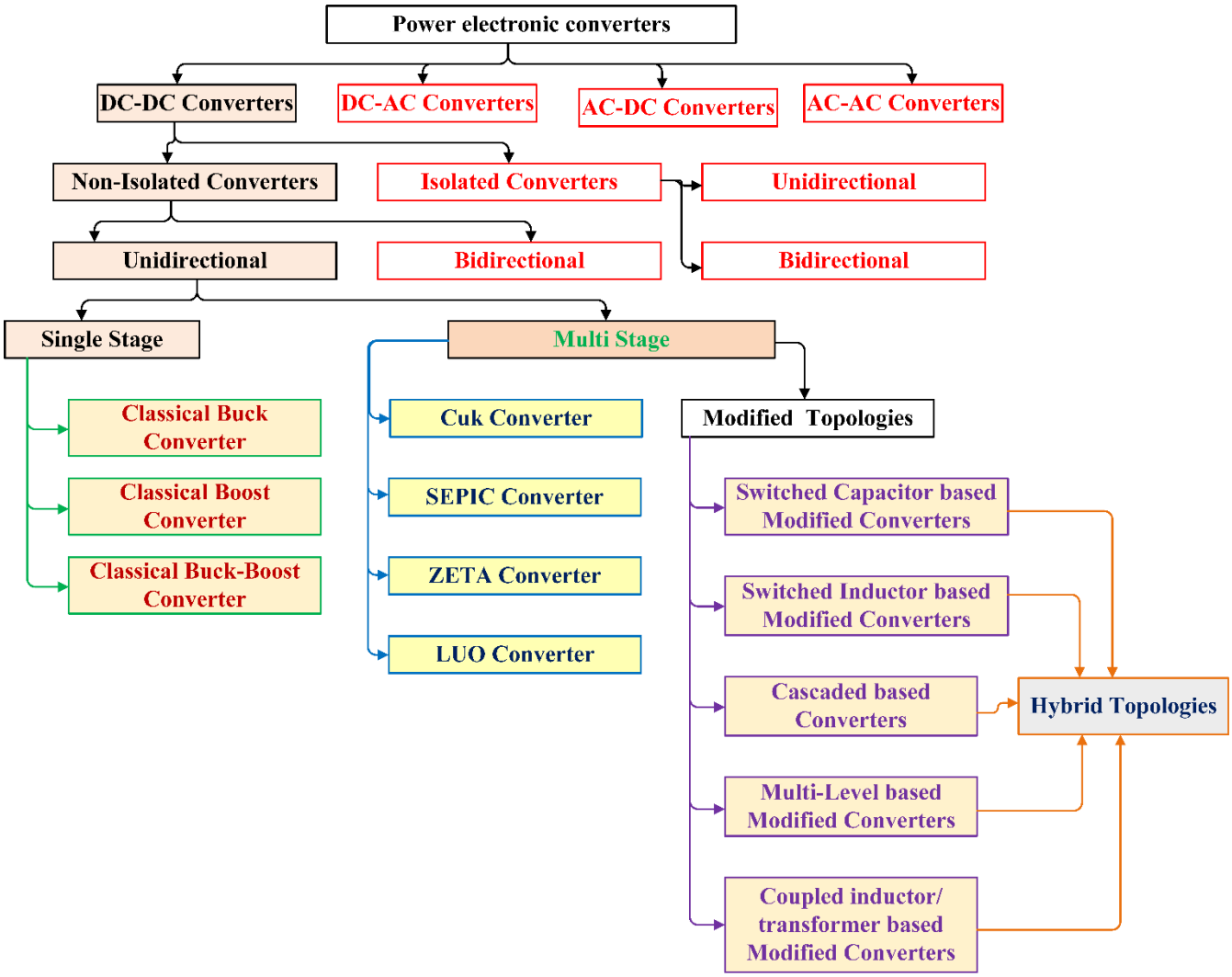

FIGURE 5. Classification of converters focusing on unidirectional high gain converters.

FIGURE 6. Generalized structure of the cascaded converter.

as common or floating grounds. Electrical isolation exists between the input and load terminals of an isolated converter. Various articles have proposed a unidirectional DC-DC converter with high gain and high efficiency for various applications like renewable energy and EV. These converters are also appropriate for achieving the high voltage demand of EV charging applications. As illustrated in Fig. 5, isolated and non-isolated converters are categorized as unidirectional and bidirectional converters. Furthermore, the non-isolated unidirectional converter subsects into single-and multistage conversion converters.

Single conversion converters include buck, boost, and buck-boost converters. Cuk, SEPIC, and ZETA converters are two-stage conversion converters. These converters are the product of the crossbreeding of two conventional converters and are not recommended for high-gain applications due to the switches' high component rating and duty ratio.

The voltage gain obtained by these converters can be classified as low, medium, or high. A low voltage gain is produced by derived or two-stage conversion converters, and a medium voltage gain is obtained by quadratic converters. High-voltage conversion is achieved utilizing topologies that include a coupled inductor, transformer, hybrid switched inductor (SI), and switched capacitor (SC).

B. LOW VOLTAGE CONVERSION STAGES

Low-voltage boosting converters are formed by joining two conventional DC-DC converters; hence they are considered to be two-stage converters. The boost and buck converters form

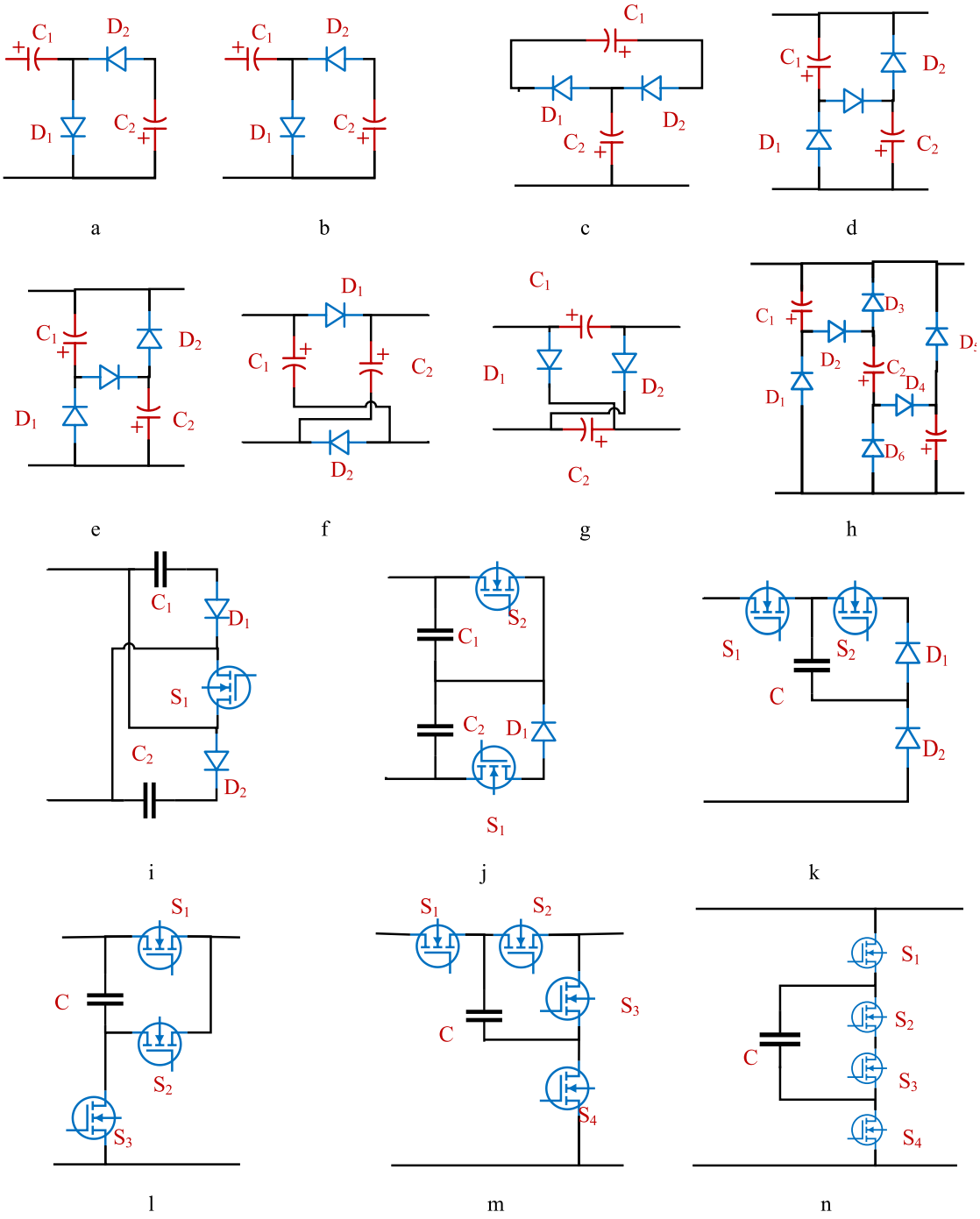

FIGURE 7. Various switched capacitor networks (a-h) uncontrolled switched capacitor structure, (i-n) controlled switch-based switched capacitor structure.

the Cuk converter, which generates a step-up/down-inverting output. The single-ended primary inductor converter (SEPIC) produces a non-inverting step-up/down that is formed from the conventional boost and buck-boost converters. Zeta converter is another topology derived buck-boost and buck converter to produce noninverting step-up/down output.

C. MEDIUM VOLTAGE CONVERSION STAGES

The gain obtained by the conventional converter does not match the demand for moderate- or high-voltage requirements. Cascaded topologies have been developed to address this gap. Many generalized constructions of the converter cascading is depicted in Fig. 6.

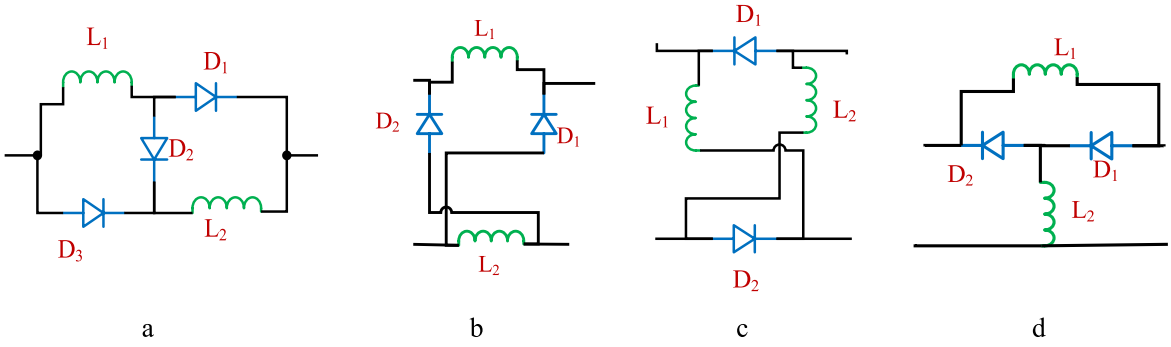

FIGURE 8. (a-d) Uncontrolled switch based switched inductor structures.

Due to the increased number of switches, inductors, capacitors, and diodes, a high voltage ratio can be reached at the cost of robustness. On the other hand, losses increase due to more components are used and thus efficiency is reduced. Quadratic converters have been designed to alleviate the drawbacks of the cascade converter; however the primary problems include voltage stress across the controlled switches, low efficiency, and additional complexity.

D. HIGH VOLTAGE CONVERSION STAGES

The gain conversion ratio of high voltage step-up converters is high by combining basic DC-DC converter with one or more voltage boosting networks. The voltage boosting stages utilize a switched capacitor (SC), switched inductor, voltage lifted inductor, voltage multiplier circuits, or a combination of these circuits. The various configurations with switched capacitors with uncontrolled switches are shown in Fig. 7 (a-h). Fig. 7 (i-n) shows the topologies of switched capacitor structure based on the controlled switch.

Recently, topologies that employ hybrid switched capacitors and switched inductors have become popular. Fig. 8 shows the(a-d) uncontrolled switch based switched inductor structures. The various hybrid combinations of switched inductors and capacitors are shown in Fig. 9. (a-j). Various structures of hybrid switched inductor and switched capacitor using uncontrolled switch; Fig. 9. (k-o) Various structures of the hybrid switched inductor and switched capacitor using a controlled switch. High-voltage converters are categorized into five subsections as follows:

- Switched capacitor-based converters.
- Switched inductor-based converters.
- Transformer or coupled inductor-based converters.
- Multilevel converters.
- Luo converters.

IV. MODIFIED/ENHANCED BOOST CONVERTER BASED TOPOLOGIES

The typical boost converter is appealing due to its simple design, grounded switch, and simple operation for a high voltage gain. The greatest limitation vehicle applications, leading to an extend/derived/modified boost converter structure. This develops a new topology of quadratic boost converter by cascading voltage gain cells for large voltage gain. Many modified DC-DC boost converters like cubic boost, quadratic boost, cascaded inductor, integrated inductor, switched inductor switched capacitor, multi-phase, multi-level interleaved, and tapped inductor, have been reported in the literature [65], [66], [67], [68], [69], [70], and are presented in Fig.10. Voltage stress across the power electronic switch affects the efficiency of the converter. As a result, the typical boost converter is incapable of reaching the needed high gain. Highly efficient converters bridge sustainable energy with electric vehicles.

A. QUADRATIC BOOST CONVERTER (QBC) BASED TOPOLOGIES

QBC shown in Fig. 11 (a) [71] is a non-isolated converter that operates in low-power high-step-up applications. QBC, like other comparable high gain topologies, suffers from large switching and conduction losses. There are several soft-switching strategies available for DC-DC converters. Coupled inductors are attracting much attention among all the zero-voltage transitions (ZVT). Quasi-resonant and semi-quasi-resonant networks resulting in low-output voltage ripples have been reported in the literature. In a conventional QBC, the diode conduction loss contributes more to the overall losses. A significant reduction in diode conduction loss, switching loss, input current ripple, and adaptive tuning of the duty cycle for switches were the major contributions of this study [71]. A hardware model was developed for 250 W of output power, operating at 100kHz switching frequency with an efficiency of 95.75%.

Fig. 11 (b) depicts a quadratic boost converter (QBC) with quadratic voltage gain, continuous input current, low ripple, a single switch, and low capacitor stress [72]. The traditional boost converter yields a voltage gain of ten at an extraordinary duty ratio, which is not experimentally conceivable. A high duty ratio causes significant current stress on power electronic switches, resulting in decreased efficiency and increased reverse recovery issues. Switched capacitor

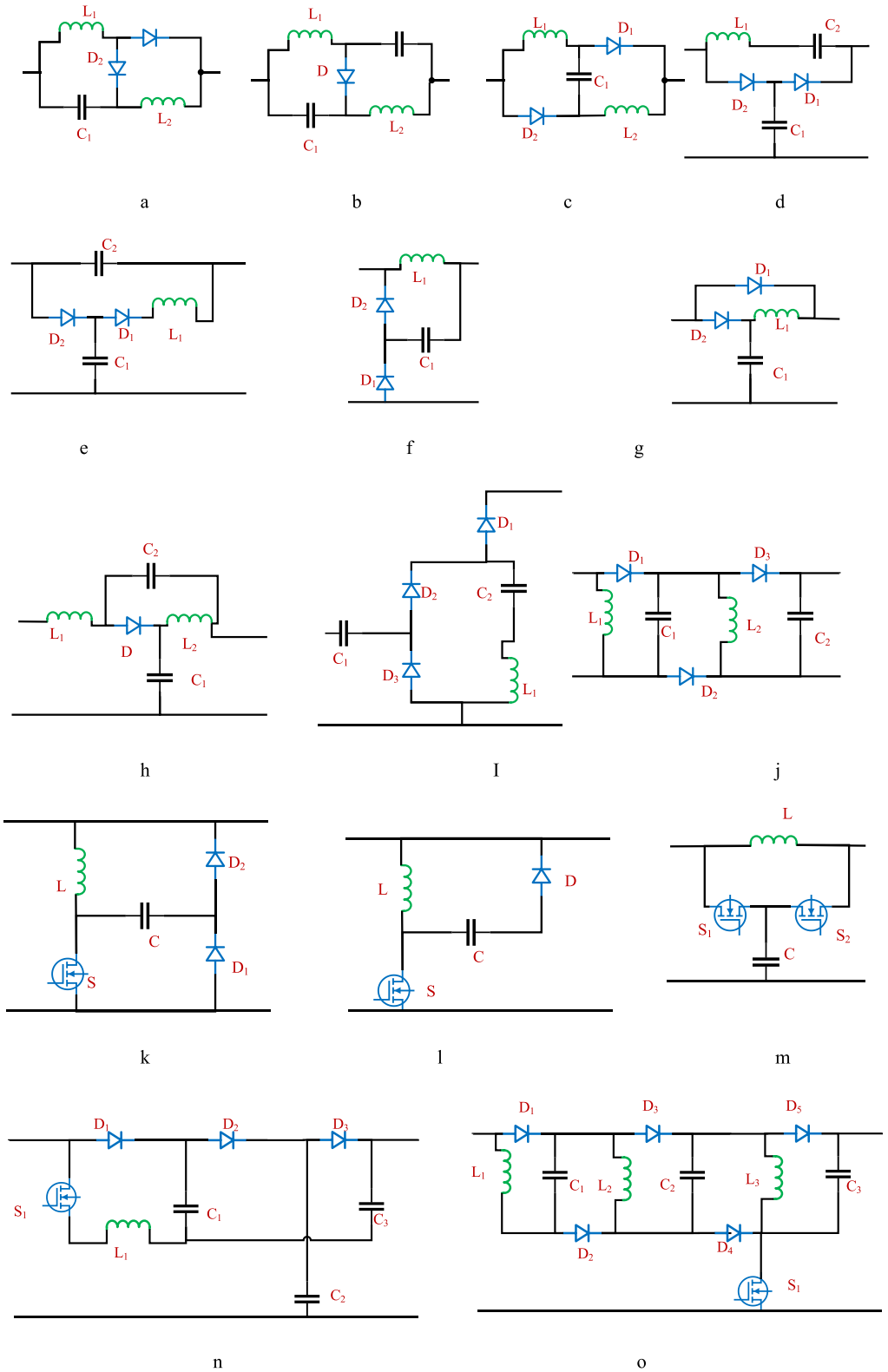

FIGURE 9. Hybrid structures of the switched inductor and switched capacitor (a-j) using an uncontrolled switch (k-o) with a controlled switch.

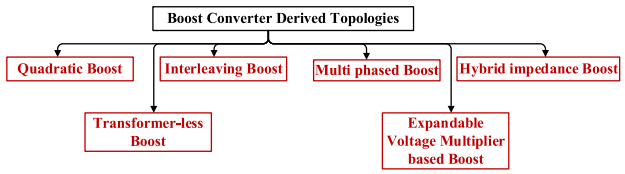

FIGURE 10. Boost converter derived topologies.

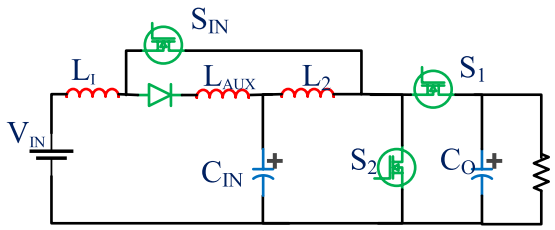

(a)QBC derived from CBC [71]

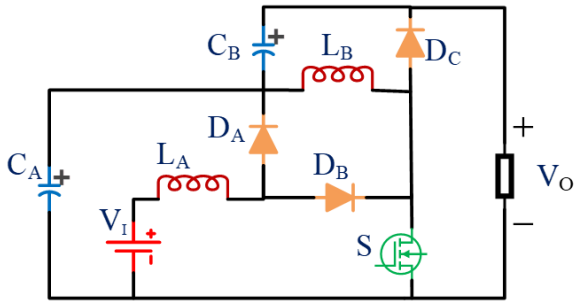

(b)QBC for Quadratic gain [72]

FIGURE 11. Quadratic boost converter.

systems offer improved voltage gain but poor regulation. The prime contributions of the article are as following:

1. Lower voltage stress on the DC capacitor in QBC.
2. A constant input current with minimal ripple aids in the reduction of the input filter capacitor size.
3. Comparative analysis with ripple factor, voltages stress, efficiency, and bode plots
4. Continuous and discontinuous conduction modes with inductor.

The major goal is to keep a steady input current on the capacitor with four reactive components and a single switch under reduced voltage stress. Modeling of the converter with small signals and DCM analysis were performed. The dynamic response of the converter during closed-loop operation, in which the output voltage tracks the set voltage independent of load or source disturbance. When the input voltage was 40V and the duty cycle was 0.6, the experimental output voltage was 237V at the output power of 200 W.

B. INTERLEAVING BOOST CONVERTER-BASED TOPOLOGIES

The benefits of interleaving converters are very minimal input-current ripple, convenient energy-storing devices, and high power-handling capability. A modified version of the interleaving converter is presented in Fig. 12. (a) [73], which employs two connected inductors and a voltage-multiplier cell. For lower voltage stress on switching devices and also for reduced ripple current, the input-side coupled inductor is responsible. High voltage gain is achieved by the two coupled inductors connected in series at the output. Also, these couple inductor helps in achieving low voltage stress on MOSFET switch. Low voltage-rated switching devices reduce switching and conduction losses. To eliminate reverse-recovery concerns, the energy accumulated in the leakage inductance is recovered with the help of output diode. To decrease the switching losses, the ZCS guarantees that the power electronic switches are switched on at zero current. To attain desired power level in medium and high power applications and parallel converter structures are preferred due to the limitations of other topologies. The voltage spikes are generated by the leaking inductance. these causes high voltage stress across the switch. The merits of paralleling converters are thermal distribution, increased power, reduced current stress on the diodes, and minimized size of power semiconductor switches. Interleaving methods minimise the size of the input filter. Two converter topologies are provided in [74], as shown in Fig. 12. (b)&(c) and the gain of two converters are Vo=(n+2) Vin/(1-D) and Vo=(n+4) Vin/(1-D) respectively. The coupling factor of all coupled inductors used was unity. At 100kHz switching frequency, the interleaved converter's experimental efficiency was 98 percent, its output power was 400 W, and its output voltage was 400V.

C. EXTENDABLE VOLTAGE MULTIPLIER CELL TECHNIQUES

A DC-DC step-up converter using an expandable voltage multiplier cell with soft switching [75], as shown in Fig.13.(a) achieves high gain. The converter achieves reduced voltage stress across the switches and diodes due to the arrangement of coupled inductors and voltage multiplier cells. This eliminates the reverse recovery problem. The proposed converter was validated using a laboratory prototype rated at 500 W at 40V input and 380V output. Compared to other converters, ultra-high gain has been achieved using minimal switches and components. Voltage stress is lowered on the capacitor and inductor size. The theoretical and experimental efficiencies of the converter are 97.23% and 96.63% at 500 W, respectively. High gain resonant coupled inductor-based expandable converter ensures soft switching for all switches and provides high gain.

The coupled inductor was presented in [76] to produce a high voltage gain, as shown in Fig. 13. (b). The circuit consists of two windings. One winding is responsible for the ZCS of the switches and diodes, while the other is used for voltage lifting/ boosting. The high voltage gain output voltage is obtained at a lower duty ratio for the main switch, which reduces the conduction loss. With an input voltage of 30V, an output voltage of 360V, and a duty ratio of 39%, an efficiency of 95.34 % was reported. The switching

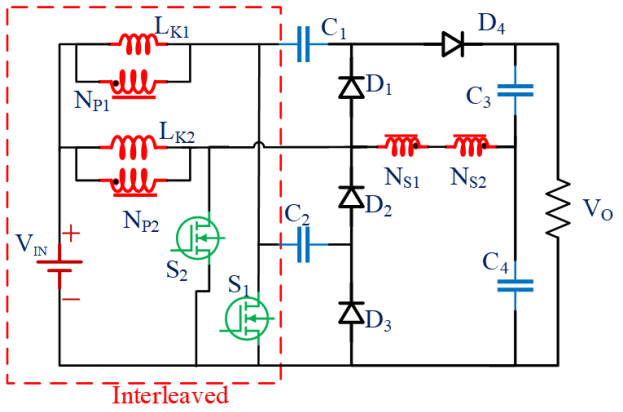

(a) Modified interleaved boost converter using 2 coupled inductors [73]

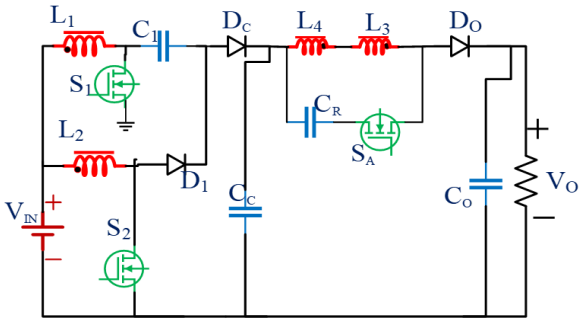

(b) Interleaved Boost converter for medium and high-power applications [74]

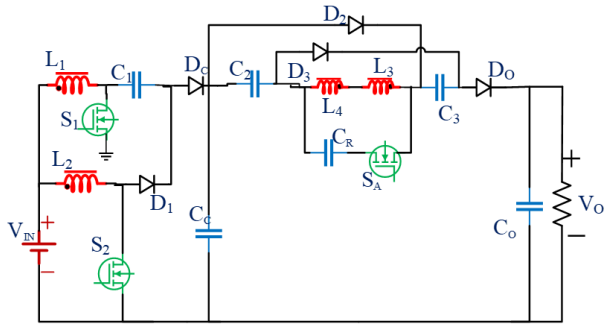

(c) improved interleaved converter [74]

FIGURE 12. Interleaved boost converter topologies.

frequency was 100kHz and the resonating frequency was 130kHz. Soft switching in high gain converters can be achieved by

1. Inductor method (high voltage stress on semiconductor devices).
2. Voltage multiplier or switched capacitor (increased components, size, and cost) Poor voltage regulation)
3. Cascade structure (high voltage stress on switches is inevitable)
4. Multilevel structure (Increased power loss and cost)
5. Resonant method.

The major properties of the converter are illustrated in Fig.13.(c) [77] are continuous and non-pulsating input current, common ground, simple, high gain control, and ease of maintenance. The voltage stress across the switch is equal to half of the output voltage. The converter's CCM and DCM operating modes are thoroughly discussed. The gain achieved in the converter is 4/(1-D) with a controlled switch and five uncontrolled switches. The duty cycle of 0.6 yields an efficiency of 94.05% for 150W output power at 30kHz switching frequency. Here the input voltage is 10V and the output voltage is 100V with a voltage gain of 10. The losses in the diode, switch, inductor, and capacitor were 65%,19%,11%, and 9%, respectively.

The bi-quadratic converter reported in [78] utilizes multiple switched inductor and capacitor networks to achieve high gain with reduced conduction loss, thereby eliminating core saturation with improved efficiency. The topology in Fig. 13. (d) is formed with the n-stage SI and SC network. The experiment was conducted for n=2 with an output voltage of 600V, power of 500 W and 50kHZ switching frequency. The effect of parasitic components is studied and reduced using SiC semiconductor switches. The efficiency obtained was 95.48% at 500W power. The experiment was carried out with an input voltage of 48V, and the observed output voltage was 650V at a 50kHz switching frequency. This converter's primary features are a low duty cycle of the switches, lower current stress, and enhanced efficiency. Other enticing aspects of the converter include the use of a single control signal and a single driver.

D. MULTI-PHASE MODIFIED BOOST CONVERTER

The batteries are the source of electrical power in the EV system. The use of high voltage-rated energy-storing batteries leads to a raise in cost, size, weight, low current, and high power density. The widespread use of public charging stations enhances efficiency, longevity, accessibility, dependability, and costs.

The interleaved structure [79] reduce the load voltage and line current ripple. To overcome the issues of high power density, conversion efficiency, and current ripple, IBCs are used for high power applications due to their low components, increased power rating, decreased element sizing, dynamic response, and high conversion ratio. The auxiliary resonant circuit can eradicate the issues related to hard switching effectively. Because of the soft switching, the converter may function in both continuous and discontinuous conduction modes with no circulating currents. Further, the voltage and current stress of the switching devices are reduced. This leads to higher switching frequencies, which reduces power loss and increases efficiency.

For EV applications, a soft switched interleaved boost converter with an auxiliary resonating circuit is used as shown in Fig. 14. Several phases can be connected according to the requirement. All the phases are identical with shifted control signal by simple PWM control technique at similar switching

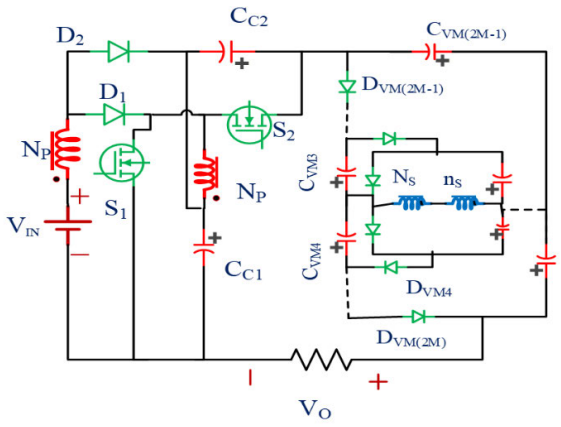

(a) Boost based expandable voltage multiplier cell with soft switching [75]

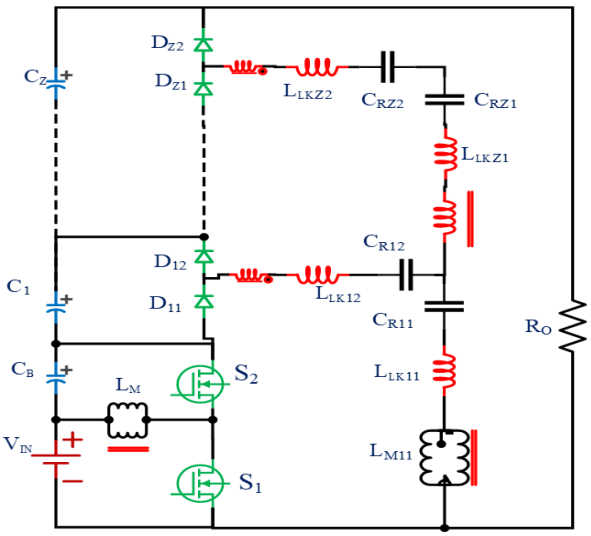

(b). Boost deriver expandable multi-winding coupled inductor [76]

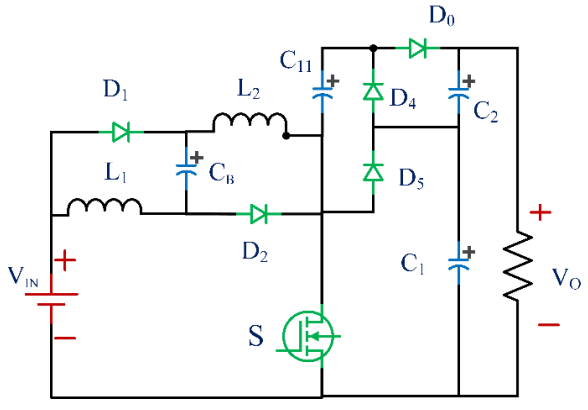

(c) Expandable hybrid switched inductor based Boost converter [77]

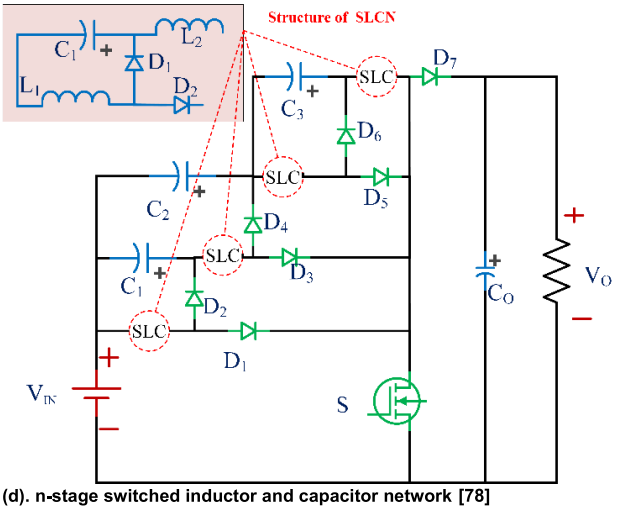

(d). n-stage switched inductor and capacitor network [78]

FIGURE 13. Extendable voltage multiplier cell techniques based boost converters.

frequency and duty ratio. The converter may operate with constant input, not alone from the grid but also from energy storage systems, renewable energy sources such as solar PV, wind, and so on. The simulation studies were carried out with the PSIM platform for 8.2kW power and obtained 97% efficiency. The experimental validation was carried out with 1.0kW power and efficiency was 98.78%.

The excellence of the converter is listed below:

1. Voltage gain is enhanced, component count is lowered, and voltage stress is minimised across semiconductor devices.
2. The built-in three-winding transformer provides greater freedom in raising the voltage gain to the optimum level.
3. The 3rd winding of the built-in transformer performs the trans-inverse operation so, that the turns ratio is lower than unity.

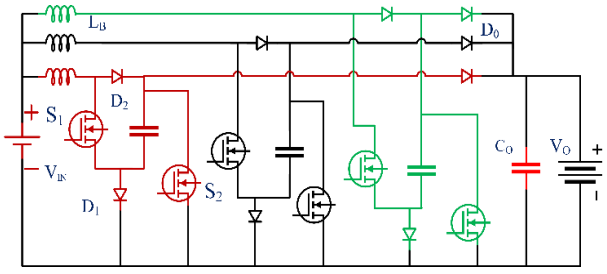

FIGURE 14. Boost converter with multi-phase modification [79].

4. Built-in transformer helps in reducing the size of the core as well as core saturation is evaded.
5. The quasi-resonant operation allows the switch to operate at reduced switching losses.
6. The input filters decrease the ripple in the input current.

E. TRANSFORMERLESS BOOST CONVERTER

A transformerless boost converter (TBC) was developed in [80] for high gain with less stress across devices as illustrated in Fig. 15. (a). High voltage gain with lower voltage stress across devices, simplified control, and improved efficiency are the major benefits. The proposed transformerless boost converter circuit derived from the traditional switched inductor-based boost converter in that diodes have been replaced with a capacitor and a controlled switch. Without increasing the component count, a high er gain is achieved compared to Simple Interleaved Boost Converter (SIBC). The power electronics switch is intended to operate concurrently, sharing the voltage to be handled and decreasing voltage stress across the components. The common ground is ensured for the load and source. A gain of 10 V was obtained with an efficiency of 92.43% at 500 W output power. The average current through any capacitor was zero. The shortcoming of this converter is that the capacitor is connected directly to the source during mode-1 operation through diode D_a and switch S_b. As a result, the transient peak current passes through the capacitor.

A non-isolated converter using a dual switch with a switching capacitor and common ground to achieve high gain at lower duty ratio was proposed in [81] and depicted in Fig. 15. (b). Using the four basic voltage boosting techniques, the duple switch with switched capacitor converter (DSSCC) type-1 and type-2 are generated. At medium duty cycles, these converter topologies exhibit low input current ripple and significant voltage gain. The important features of this converter topology are as follows:

1. High gain at medium duty cycle for the common ground.
2. Minimized input current ripple.
3. Device stress is less than half of load voltage.
4. Various ranges of supply variations can be addressed by a small change in the duty cycle.
5. Less number of components produces the same gain compared to the comparable topologies.

The experimental peak efficiency measured is 97% at the output power of 120W and output voltage of 220V at 50kHz switching frequency with the input voltage of 48V.

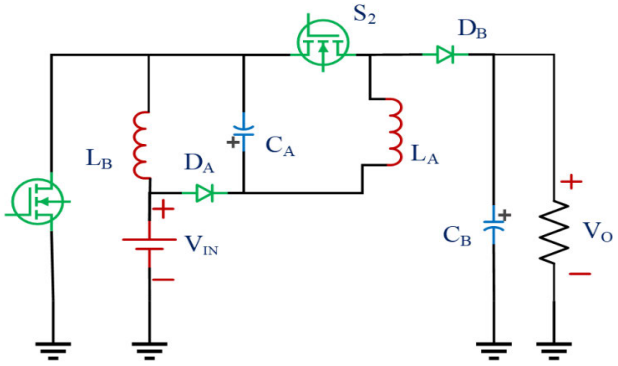

(a) Transformerless dual switch boost converter [80]

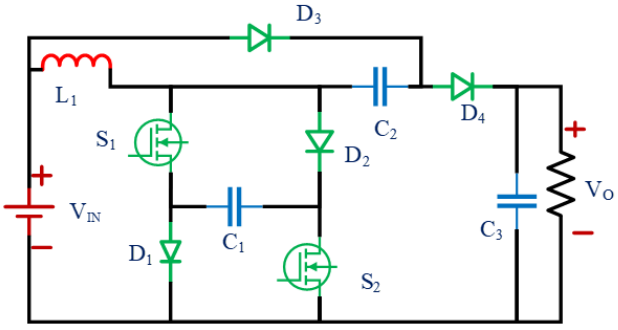

(b) Duple switch with SC converter (DSSCC) type-1 [81]

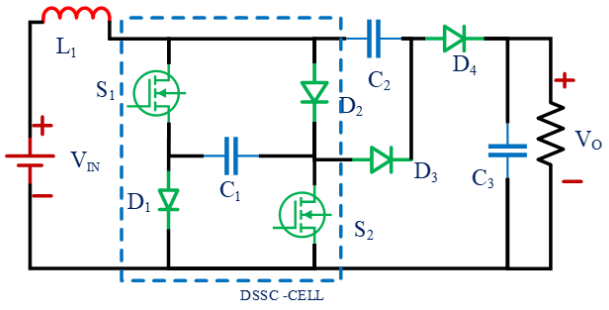

(c) Duple switch with SC converter (DSSCC) type-2 [81]

FIGURE 15. Transformerless boost converter.

F. HYBRID SWITCHED CAPACITOR AND SWITCHED INDUCTOR DERIVED BOOST CONVERTER

A hybrid boost converter with switched capacitor and switched inductor was presented in [82] illustrated in Fig. 16. (a). Controlling the switched inductor and switched capacitor independently, tackles the input current ripple. As a result, the size of the inductor is lowered in DCM operation. Also, the current stress of the components S_1, S_2, D_1, D_2, and C1 is decreased. The output voltage of 396V is obtained by applying the input voltage of 100V with a 95kHz switching frequency. The charge pump / switched capacitor is added to the circuit to improve the voltage gain without including inductors [83] as shown in fig 16.(b). The normal diodes may suffer due to dynamic losses than the controlled switches. Losses can be reduced by using silicon carbide (SiC) and gallium nitrate (GaN) power diodes. To minimize the size and weight, a common core is used for inductor windings. The voltage gains of 7.5 and 19 are obtained with D=0.5 and 0.8 respectively. The gain can be enhanced further by cascading switched capacitor cells. The experimental peak efficiency was 96%, the output power was 200 W, and the output voltage was 360V when the input voltage was 48V with a 50kHz switching frequency.

This converter architecture stands out from other reported articles for offering higher gain due to the concept of regenerative boost design by incorporating switching capacitor configuration. The topology discussed in article [84] is presented in Fig. 16. (c). The main features highlighted were low

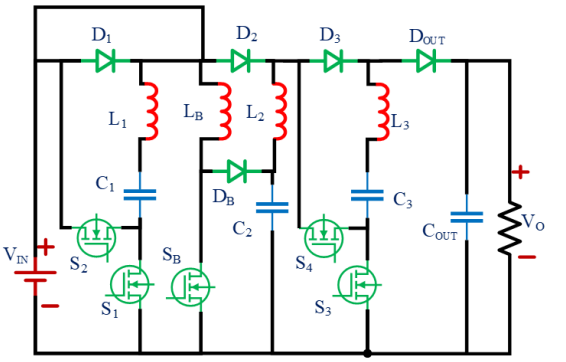

(a) Boost converter based on a hybrid of switching capacitors and inductors [83]

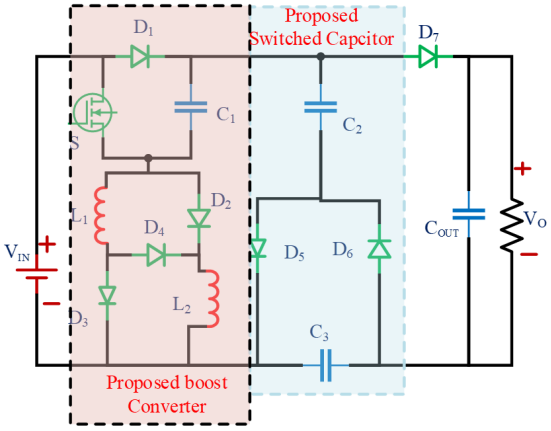

(b) Switched capacitor based modified Boost converter [83]

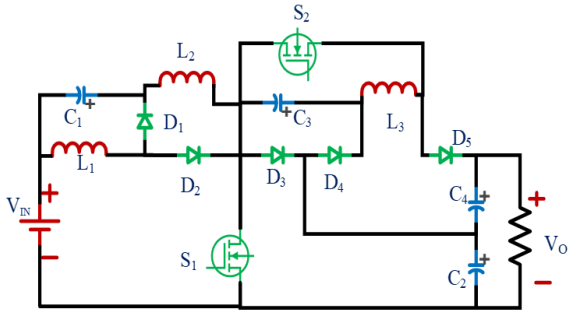

(c) Integrated switched capacitor based Boost converter [84]

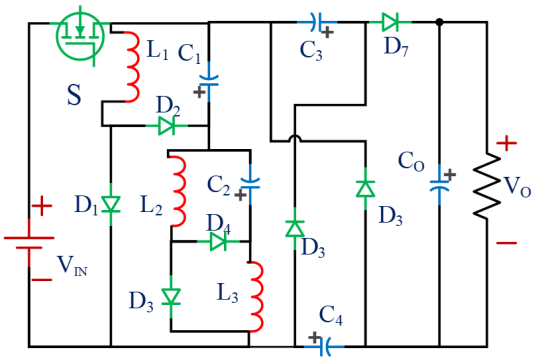

(d) Multistage ultra-high voltage gain [85]

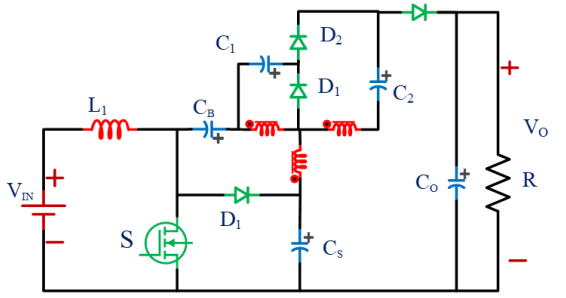

(e) Modified quasi-Z-source, n level switched capacitor [86]

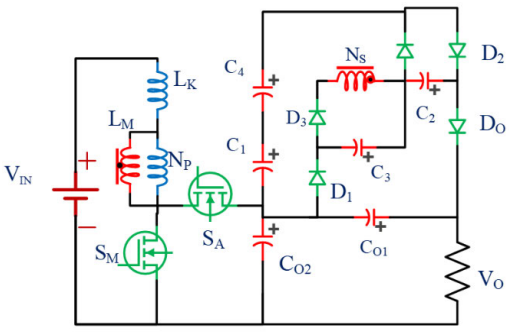

(f) Quintupler rectifier and coupled inductor [87]

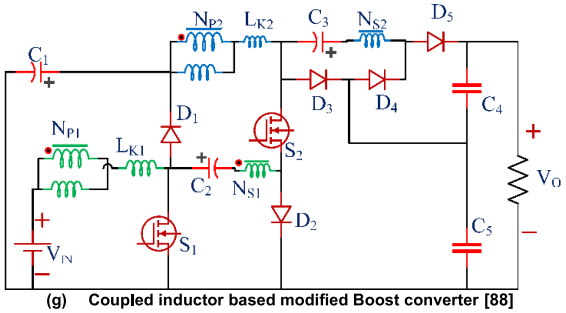

(g) Coupled inductor based modified Boost converter [88]

FIGURE 16. Hybrid boost converter with switched capacitor and switched inductor.

voltage stress, extremely high voltage gain, lower on-state resistance, and less component count for achieving better efficiency, which was confirmed through the hardware results.

Multistage ultra-high gain using switched impedance with single power switching device that operates with minimal components and high gain with low switch voltage stress is proposed in [85]. Fig. 16. (d) represents the topology. The

TABLE 5. Review of voltage gain and voltage stress expressions of boost converter derived topologies.

REFERENCE	GAIN	VOLTAGE STRESS	CONTRIBUTIONS
[72]	$G = \frac{1}{(1-D)^2}$	NR	• QBC with reduced voltage stress on a posterior capacitor. • A continuous input current with minimal ripple aids in the reduction of the size of an input filter capacitor.
[73]	$G = \frac{4+2nk}{1-D}$	$V_{S1} = V_{S2} = \frac{1}{1-\frac{D}{2}} V_{in} = \frac{1}{4+\frac{2n}{2}} V_o$ $V_{D1} = V_{D2} = \frac{1}{1-\frac{D}{2}} V_{in} = \frac{1}{4+2n} V_o$ $V_{D3} = V_{D4} = \frac{2+2n}{1-D} V_{in} = \frac{2+2n}{4+2n} V_o$	• Low duty ratio • Utilizes minimum components • Simplified control and high efficiency
[74]	Ist $G = \frac{n+2}{1-D}$ 2nd $G = \frac{n+4}{1-D}$	$V_{S1} = V_{S2} = \frac{V_o}{n+2}$; $V_{D1} = V_{D0} = \frac{2V_o}{2+2}$	• A unique interleaved soft switched boost converter with a simple auxiliary circuit. • Provision is included for the installation of additional switched capacitor cells in order to obtain larger voltage gains.
[76]	$G = \frac{5n+3}{1-D_1}$	NR	• To produce a high voltage-gain resonant converter, a multi-winding coupled-inductor is used. • Through the resonant tank, all diodes attain ZCS.
[77]	$G = \frac{4(D+(1-D))}{1-D}$	$V_S = V_{D4} = V_{D0} = \frac{V_O}{2}$; $V_{D1} = V_{D2} = \frac{V_O}{4}$ $V_{D0} = 0$	• A single-switch switched-inductor and capacitor-divided network is employed • Less a duty ratio for the switch and not using coupled inductor or transformer.
[78]	$G = \frac{1}{(1-D)^4}$	$V_S = \frac{V_s}{(1-D)^4}$; $V_{D1} = \frac{-D\,V_s}{(1-D)^2}$; $V_{D2} = \frac{-V_s}{1-D}$; $V_{D3} = \frac{D(D-2)\,V_s}{(1-D)^4}$; $V_{D4} = \frac{-V_s}{(1-D)^2}$; $V_{D5} = \frac{-D\,V_s}{(1-D)^4}$; $V_{D6} = \frac{-V_s}{(1-D)^3}$; $V_{D7} = \frac{-V_s}{(1-D)^4}$	• To achieve ultra-voltage gain, many SLCN networks are employed. • Low duty ratio
[80]	$G = \frac{2}{1-D}$	$V_{S1} = V_{S2} = \frac{V_O}{2}$; $V_{DA} = V_{DB} = V_O$	• Two diodes are replaced by a capacitor and a control switch in the switched inductor boost converter. • Control is simple, and efficiency is high.
[81]	$G = \frac{2V_{IN}}{(1-2D)}$	$V_{S1} = V_{S2} = V_{D1} = V_{D2} = \frac{V_{IN}}{(1-2D)}$	• Low source current ripple • Continuous input current • No load voltage inversion • Two switch converter
[82]	$G = \frac{2V_{IN}}{(1+D)}$	NR	• Parallel switched capacitor and boost converter • Low cost due to hybrid structure • A small inductor and volume
[83]	$G = \frac{3+D}{(1-D)}$	NR	• A moderate number of component • Improved efficiency
[84]	$G = \frac{2-D}{(1-D)^3} V_{IN}$	$V_{S1} = \frac{1-D}{2-D} V_O$; $V_{S2} = \frac{1}{2-D} V_O$; $V_{D1} = \frac{(1-D)^2}{2-D} V_O$ $V_{D2} = \frac{D(1-D)}{2-D} V_O$; $V_{D3} = V_{D4} = V_{D5} = \frac{1-D}{2-D} V_O$	• High gain at minimal duty cycles. • A voltage gain is composed of fewer components. • There is virtually low voltage stress across the switch. • Better efficiency
[85]	G $= \frac{D^3-3D^2+3D+1}{(1-D)^3}$	NR	• The active impedance network employs a single MOSFET switch. • Uses minimal components
[86]	G $= \frac{K_2K_3+K_1K_3n_1+D}{(1-D)(K_2K_3-K_1K_2n_2)}$	$V_S = V_{SD4} = \frac{V_O}{B(1-D)}$; $V_{SD1} = \frac{n_2V_O}{B(1-n_2)(1-D)}$ $V_{SD2} = \frac{(n_1+n_2)V_O}{B(1-n_2)(1-D)}$; $V_{SD0} = \frac{(1+n_1)V_O}{B(1-n_2)(1-D)}$	• It is a variant of the quasi-Z-Source Network. • Circuit for Continuous Input Current and Passive Clamping
[87]	G $= \frac{N^2+N(3+D)+D+3}{(1-D)^2}$	$V_{S1} = V_{D_1} = \frac{(1+D)V_o}{N^2+(1+N)(3+D)}$ $V_{S2} = \frac{(1+D+nD)V_o}{N^2+(1+N)(3+D)}$ $V_{D_2} = \frac{(1+N)(1-D)V_o}{N^2+(1+N)(3+D)}$ $V_{D_3} = \frac{(2+n)V_o}{N^2+(1+N)(3+D)}$ $V_{D_4} = V_{D5} = \frac{2+n1+2n2+n1n2V_o}{N^2+(1+N)(3+D)}$	• DC-DC converter with a high step-up ratio • A limited number of components • The coupled inductor's turn ratio is higher.
[88]	$G = \frac{1+N(D+2)}{1-D}$	NR	• Effective recycling of energy stored in the coupled inductor • ZVS switching at turn on. • Fewer switching losses and improved power density

*G- gain; N- number of voltage levels; D-Duty ratio; k- coupling coefficient; V_{in}= input voltage V_0- output voltage; V_S - voltage stress across switch; V_D- voltage stress across diode; NR- Not Reported

TABLE 6. Comparison of boost converter derived topologies- based on the component count, input voltage output voltage, gain, efficiency at peak load.

Reference (s)	Element's count	T	Input voltage (V)	Output voltage (V)	Gain reported with switching frequency	Peak η at Reported Power	cost ($)	complexity
[84]	L-4; C-5; S-2; D-5	16	24	350	G=15 at Fs=20kHz	94.58% at 500W	111.6	**
[75]	L-2; C-7; S-2; D-4	15	40	380	G=10 at Fs=100kHz	96.63% at 500W	105.6	***
[87]	L-2; C-5; S-2; D-5	14	15	600	G=40 at Fs=50kHz	95.2% at 250W	94.8	**
[80]	L-2; C-2; S-2; D-2	8	NR	NR	G=10 at Fs=NR	92.43% at 500W	86.4	**
[78]	L-4; C-4; S-1; D-7	16	48	650	G=14 at Fs=50kHz	95.48% at 500W	73.2	**
[79]	L-1; C-1; S-2; D-2	6	40	140	G=4 at Fs=25kHz	98.78% at 600W	90	***
[85]	L-3; C-5; S-1; D-7	16	20	650	G=33 at Fs=50kHz	NR at 200W	58.8	**
[72]	L-2; C-2; S-1; D-3	8	40	250	G=6.25 at Fs=50kHz	NR at 200W	87.6	**
[83]	L-2; C-4; S-1; D-7	14	48	360	G=8 at Fs=50kHz	96% at NR	56.4	**
[82]	L-4; C-3; S-5; D-5	17	100	396	G=4 at Fs=95kHz	95% at 600W	73.2	***
[81]	L-1; C-3; S-2; D-4	10	NR	220	NR at Fs=50kHz	NR at120W	98.4	**
[77]	L-2; C-4; S-1; D-5	12	10	100	G=10 at Fs=30kHz	94.05% at 150W	153.6	**
[74]	L-4; C-4; S-4; D-3	15	48	400	G=8.33 at Fs=100kHz	98% at 400W	73.2	***
[76]	L-4; C-4; S-2; D-4	14	20-30	NR	G=18 at Fs=100kHz	NR at 260W	70.8	***
[88]	L-3; C-6; S-2; D-5	16	30-40	400	G=10 at Fs=100kHz	96.43% at 400W	139.2	***
[86]	L-2; C-5; S-3; D-1	11	28-48	380	G=13.57 at Fs=4Hz	95.53% at 200W	104.4	**
[73]	L-4; C-4; S-2; D-4	14	20	400	G=20 at Fs=40kHz	93.2% at 400W	109.2	***

* L-No. of Inductors; C- No. of Capacitors; S- No. of switches; D- No. of Diodes; T-Total Components used; G-Gain; Fs-Switching Frequency; NR- Not Reported; *complexity level-low, ** complexity level-moderate; *** complexity level -high; **** complexity level-extra/ultra-high

experimental validation was performed at a rated power of 200W and 650V output voltage at a switching frequency of 50kHz. The fabricated prototype with 20V input and 63% duty ratio. The losses in the switch and diode contribute 69% of the total losses. Here, the n-stage structure uses 4(n+3) components. The article's discussion was

made for n=1 so the converter uses 16 components in total.

Modified quasi-Z-source, three winding coupled inductor, and n-level switched capacitor for regulated output voltage high gain converter is presented in [86] as shown in Fig. 16. (e). The main advantages of this converter are its high gain, constant input current, reduced voltage stress on switch passive clamping circuits, and improved efficiency. The stacked n-level switched capacitor ensures high gain, high efficiency, and a low turn ratio of coupled inductors. Voltage boosting / enhancement may be accomplished by varying the turns ratio of a connected inductor, the number of layers of switched capacitors, and the duty cycle. The duty ratio of the converter can be varied from 0.1 to 0.6 which avoids the extreme duty ratio. The experimental coupling coefficients are k1=0.992; k2=0.997; k3=0.995. The voltage gain is unaffected by the leakage inductance. The experimental efficiency is 98.43%, the output power is 200W with an input voltage of 28V and output voltage of 380V and the attained gain is 13.57.

The converter proposed in [87] has distinguishing attributes include minimal voltage stress on the power electronics switching devices, common ground, continuous input current and ultra-high gain. Fig. 16. (f). shows the topology of the modified boost converter. The coupled inductor is an optimal method of voltage boosting since a single magnetic core can have two or three coils. Nevertheless, the number of turns is determined by the required gain. Cascading two classical boost converters (CBC) leads to a quadratic boost converter (QBC). The two switches of the converter operate simultaneously so that the voltage is shared by both switches thereby voltage stress across the switches is reduced. The experimental output power is 250W, the output voltage is 600V, and the input voltage ranges between 15 and 30 volts. The obtained experimental gain is 40.

The voltage gain can be obtained by combining a quintupler rectifier and coupled inductor for the reduced duty ratio as shown in Fig. 16. (g). [88]. In this structure, the leakage flux is recycled to the capacitor by the axillary switch to enhance the gain. The active clamp and huge inductor also address the voltage spikes and voltage stress across MOSFET. This active clamp enables the soft switching of MOSFET. The experiment efficiency is 96.43%for the output power of 400W operating at 100kHz switching frequency.

Table 5 presents the gain and voltage stress across the switch and diode of various converter topologies discussed under derived/enhanced/modified boost converter topologies. The gain in any converter topology for EV DC fast charging application is essential. The voltage stress across the regulated and uncontrolled power electronic switches must be reduced for enhanced efficiency with high gain. The voltage stress on the switches is determined by their position in the converter topology.

Table 6 compares various boost converter topologies based on the component count, input voltage, output voltage, voltage gain, switching frequency, and peak efficiency at the rated power, cost, and complexity level. The comparison helps us to find the cost-efficient, less complex more efficient converter topology that suits sustainable EV charging Applications.

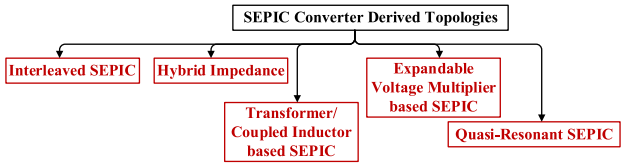

FIGURE 17. Classification of SEPIC converter derived topologies.

G. INFERENCES

The coupled inductor lowers the needed number of switching devices and ripple current. Switching and conduction losses are reduced while using low-rated switching devices. The energy stored in the leakage inductance is recycled through the output diode during reverse recovery. ultra-high gain is achieved with the use of minimal switching components. The converter's duty cycle needs to be kept below 50% for high efficiency. It is necessary to resolve the problems caused by hard switching of the switching devices by employing soft switching techniques. The converter should be capable of operating in both continuous and discontinuous modes with no circulating currents. Without any circulating currents, the converter should operate in both continuous and discontinuous modes. Devices made of SiC and GaN can boost efficiency while reducing loss. The converters are expected to have minimal voltage stress across the switches, continuous input current, common ground between input and output, and ultra-high gain without raising component count.

V. MODIFIED/ENHANCED SEPIC CONVERTER BASED TOPOLOGIES

The SEPIC converter has drawbacks such as high input ripple current, voltage stress, switching losses, and reverse recovery problems. The quasi-resonant operation would minimize voltage stress on the power electronics switches and therefore losses reduce. The inherent feature of the continuous input current of the SEPIC converter attracts interest. To achieve more gain, modification on SEPIC-based converters came into existence. The various topological categories of the SEPIC converters are shown in Fig. 17.

A. INTERLEAVED ENHANCED SEPIC CONVERTER

ZVS implemented a modified SEPIC converter working at a switching frequency is high was discussed in [89]. The topology proposed is presented in Fig. 18. (a). The increased voltage gain and decreased voltage stress of the switches are important advantages of the DCM converter. When the duty cycle is close to unity, the discharge time for the inductor decreases and saturates effortlessly. Capacitor-switched circuits can provide high power density as no magnetic components are included. However, power density and efficiency are reduced when operating at high current transients. In high

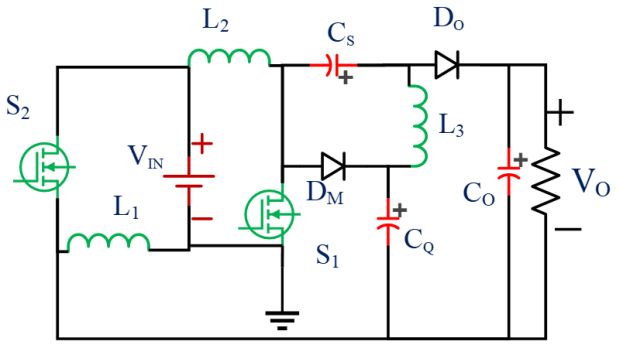

(a). ZVS implemented a modified SEPIC converter [89]

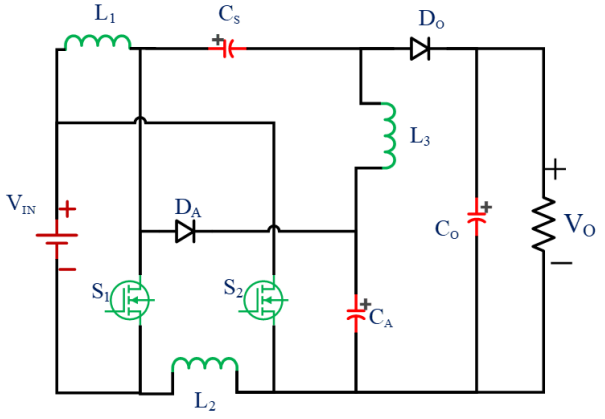

(b). Coupled inductor-less SEPIC converter [90]

FIGURE 18. Interleaved enhanced SEPIC converter.

frequency designs, switching loss associated with hard switching is unavoidable. Therefore, soft switching reduces switching losses and allows the converter to work on high frequency applications. At the rated output power of 36W, the converter's experimental full load efficiency is 91.8 %.

The coupled inductor-less SEPIC based topology was proposed [90] as shown in Fig. 18. (b). Lower voltage stress on the switches, constant input current, non-inverting output voltage, high efficiency, and high gain are some of the benefits of employing a non-coupled inductor-based SEPIC converter. Since coupled inductor is not employed, no clamp circuit is required. The two switches of the proposed circuit use the same gate pulse. As a result, adjusting the duty cycle yields a wide range of output voltage. The converter is simple to control. The 40kHz switching frequency, the duty cycle is 74.2%. The efficiency achieved is 93% at 200W output power.

B. COUPLED INDUCTOR / TRANSFORMER-BASED SEPIC CONVERTER

Transformer based SEPIC converter along with passive components for improved performance in terms of high gain, highly efficient, low voltage stress, and soft switching characteristics is proposed in [91] and is shown in Fig.19. (a). The key contributions are partially interleaved structure for

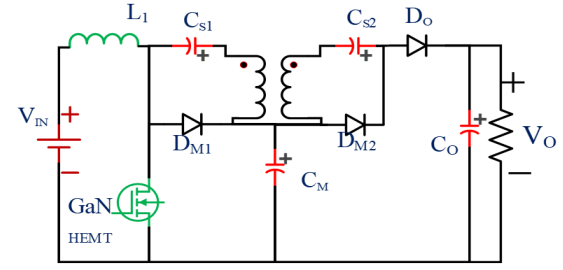

(a). Transformer based SEPIC converter [91]

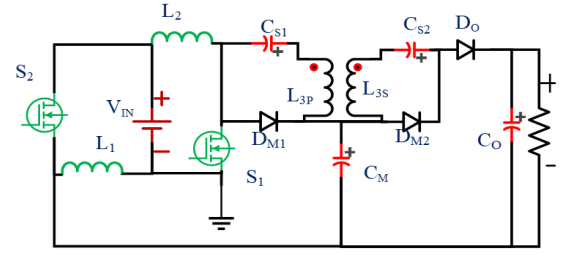

(b). High frequency SEPIC converter [92]

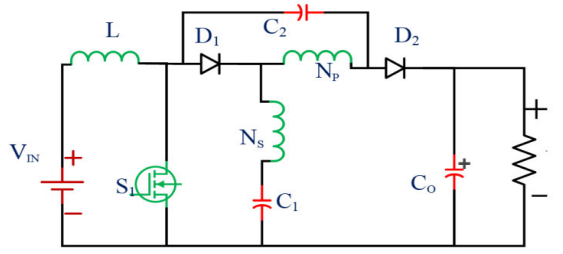

(c). Switched capacitor-based SEPIC converter [93]

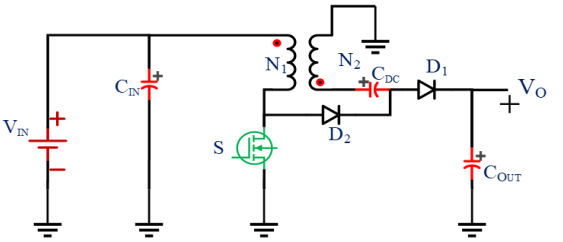

(d). Improvised coupled inductor based SEPIC converter [94]

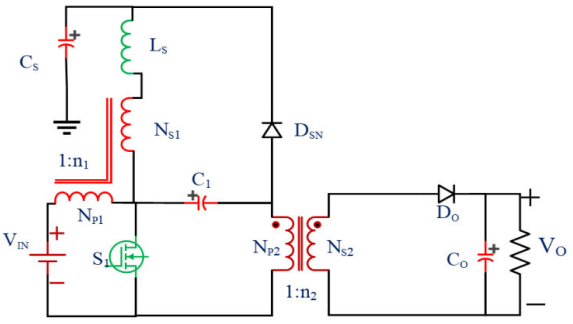

(e). Isolated SEPIC DC-DC converter [95]

FIGURE 19. Coupled inductor / transformer-based SEPIC converter.

low parasitic capacitance and leakage inductance, improved power density, and magnetic component optimization. The interleaving approach is the best way to decrease leakage

inductance. The switched capacitor generates large current transients, lowering the power density and efficiency of the converter. The method of soft switching of the converter has become a prominent characteristic in the converter's performance evaluation. Devices like SiC and GaN have the merits of fast switching and low conduction losses, making the converters perfect for high power and high frequency applications. The experimental efficiency obtained is 93.1% for the 80W output power.

High frequency SEPIC operating in DCM (discontinuous conduction mode) is proposed in [92] as shown in Fig. 19. (b). The switched inductor, coupled inductor, and resonant cell for zero voltage switching (ZVS) enable this converter to achieve high voltage gain. The full load efficiency in the experiment is 93.4 %. With a duty ratio of 50%, the voltage gain is 15. The switching frequency is 500kHz.

The absence of magnetic components produces high gain with high power density by switched capacitor technique proposed in [93] is shown in Fig. 19. (c).

The distinguishing features of this converter include:

1) By reducing the magnetic turns ratio, the converter's voltage conversion ratio is.
2) Wide control range of duty cycle.
3) Continuous input current.
4) Because of the existence of a capacitance in the main coil of the inductor, there is no core saturation caused.

To simplify the analysis, the following assumptions are

1) The parts are all perfect.
2) The voltage across the capacitors is assumed constant.
3) The coupling coefficient is one so leakage inductance is zero.

The reported efficiency is 92% for the rated output power of 325W. For a 48V input, the output voltage is 400V.

SEPIC DC-DC converter with improvised coupled inductor for high gain application was proposed in [94] as shown in Fig. 19. (d). For medium voltage applications, the coupled inductor is better suited for high voltage with minimal power losses. Because the voltage stress on the switches is minimized, which enables low-powered switches with low turn-on resistance, making the converter efficient and cost-effective. The indigenous contributions of the article are:

1) The converter is designed for renewable energy applications, with a nominal input voltage of 40V and an output voltage of 400V at 400W.
2) The converter was subjected to CCM and DCM analyses.
3) High voltage gain.
4) Enhancing the design of the inductive coupling to eliminate leakage inductance and voltage spikes across the switch.

The highest reported peak efficiency is 96.2 %, with a full load efficiency of 95.2 %. The voltage gain claimed is close to 10.

It is reported that a topology based on an isolated SEPIC DC-DC converter paired with a lossless snubber circuit is used in [95] as shown in Fig. 19. e. The isolation is due to the coupled inductor which adds merits of galvanic isolation and high gain. The snubber circuit compresses the switch's voltage stress to a low voltage. The input voltage is 48V, the output voltage is 200V, the maximum power is 100W, and the switching frequency is 50kHz.

C. EXTENDABLE VOLTAGE MULTIPLIER CELL TECHNIQUES

Converter [96] uses a single switch for high gain conversion but the voltage stress across the switch is low. Fig. 20. (a). shows the SEPIC-based extendable voltage multiplier cell techniques. Also, the input current is continuous so, huge filters are not essential. SEPIC converter can perform buck and boost operations with the continuous input current. The experiment was conducted with an output power of 110W. The input voltage for buck operation is 22V output voltage is 18V. The input voltage for the boost operation is 25V, and the produced output voltage is 110V.For both buck and boost operation, the 33kHz switching frequency and the duty ratio for buck and boost operation are 22% and 60% respectively. The efficiency for boost operation is 97% at 18W and the overall efficiency of the converter is 93.3% at 110W.

A modified SEPIC converter employing a switched capacitor voltage double circuit [97] is shown in Fig. 20. (b). The switched capacitor delivers superior gain while exerting less strain on semiconductor switches. The modified cell preserves high quality input current, which is an important aspect of the SEPIC operating in DCM. The converter circuit reduces voltage stress on the semiconductor devices and provides more power than the literature reported. The 1000W output power prototype model was developed for experimental validation of the proposed converter. Other technical elements of the converter include an input voltage of 220V and an output voltage of 800V with a switching frequency of 50kHz.

D. HYBRID SWITCHED CAPACITOR AND SWITCHED INDUCTOR-BASED SEPIC CONVERTERS

An isolated modified SEPIC converter is proposed in [98] and [99]. To achieve maximum efficiency, low voltage components and lower parasitic parameters were used. Through the literature, the author has identified that the two separate inductors will have separate core losses. The study has been carried out to reduce the core losses of the magnetic elements. The feasible solution for the above-said issues was identified and addressed by integrating the two inductors in the same core as shown in Fig. 21. (a) [18], [19], [98], [99]. As a result, the core's losses and volume are minimized. At the rated load, the 36W laboratory model has an efficiency of 91.5 %.

As shown in Fig. 21. (b) For higher voltage gain, a single switch with a coupled inductor, a voltage multiplier, and an improved passive lossless clamp circuit are used is proposed in [100]. The leakage inductance of the coupled inductor ensures that the controlled switch turns on and off at zero current.

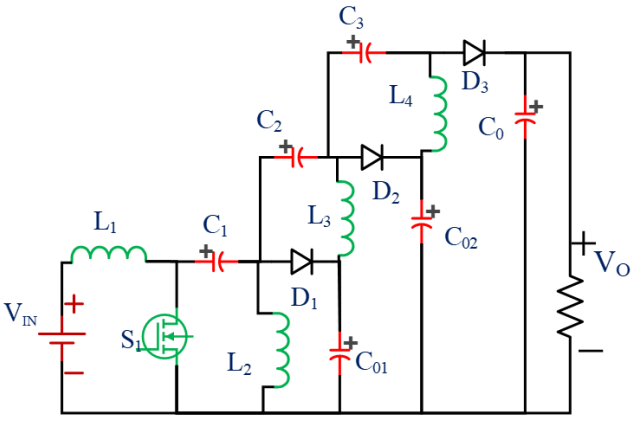

(a). SEPIC based extendable hybrid SC and SI [96]

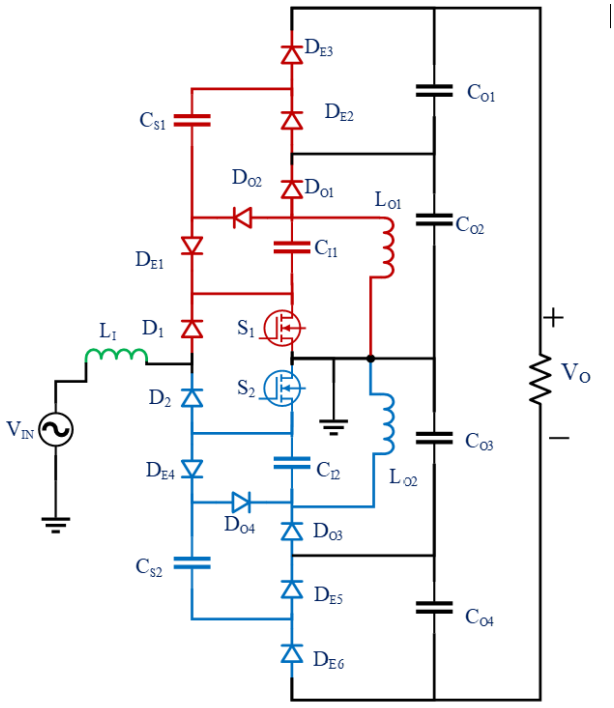

(b). Modified SEPIC converter with switched capacitor [97]

FIGURE 20. Extendable voltage multiplier cell techniques based SEPIC.

There is no issue with reverse recovery. Since coupled inductor slackens the slope of all the diodes. The experimental model is developed for the rated power of 160W at an output voltage of 200V while the input is 20V at the switching frequency of 60kHz yielding an efficiency of 97.8%.in [101] as shown in Fig. 21. (c). For many applications like DC homes, Electric vehicles, DC microgrids, etc., high gain converters are employed as a bridge. The coupled inductor or transformer based isolated topologies are bulky besides the voltage spikes introduced by them. Although isolated converters obtain significant voltage gain by modifying the inductor's turns ratio, leakage inductance is unavoidable and necessitates clamping circuits. The non-isolated converter is a more compact and efficient solution for high gain applications. Although isolated converters obtain significant voltage gain by altering the turns ratio of the inductor, leakage inductance is unavoidable and necessitates clamping circuits are:

1) Reduced control complexity due to the usage of a single switch.
2) Input current is continuous.
3) High voltage conversion ratio.
4) Maximum input source utilization.

The experimental validation provides 91.4% efficiency at 100W output power for transforming 24V input to 172V output.

The converter [102] is shown in Fig. 21. (d). For high gain and constant input current, it has two voltage multiplier units and a coupled inductor. The passive clamp circuit is utilized for voltage gain as well as to minimize voltage stress on the switch by reducing the coupled inductor's leakage inductance. As a result, the controlled switch's conduction loss is reduced. The lowered voltage stress on the diode mitigates the reverse recovery problems. The input current should be continuous and ripple-free for improved input power regulation. The suggested converter's major advantages are high gain, minimal ripple continuous input current, and low voltage stress. The laboratory model was designed for a 245W output power. The achieved efficiency is 93.5 % for a 20V input voltage and a 300V output voltage at a duty ratio of 62 %.

SEPIC three-phase high power factored converter is shown in Fig. 21. (e), operating in DCM is presented in [103]. DCM operation delivers input current with low harmonic content that is in phase with the input voltage in the absence of any current control. The absence of bulky filters and 3rd-order harmonics free input current are the main features of SEPIC converter-based AC-DC converters The experimental model is developed for the output power of 3000W and has achieved a peak efficiency of 95.85%. For the input voltage of 220V, the output voltage obtained is 400V.

E. QUASI-RESONANCE OPERATION SEPIC CONVERTER

A modified SEPIC converter using a single switch converter is shown in Fig. 22. (a), for high voltage conversion, is proposed in [104]. Voltage multiplier cells with switched capacitors boost voltage gain while decreasing voltage stress across the power switch. Quasi resonant circuit ensures zero current switching of all the power electronics switches. The experimental validation has been carried out for 200W output power and the reported efficiency is 94.4%. The output voltage of 250V is produced for a 20V input voltage. The switching frequency is 55kHz, with a duty ratio of 55%.

Fig. 22. (b) shows the Modified SEPIC converter for high performance with inherent high gain proposed in [105]. Because soft switching reduces losses and electromagnetic interference, this converter is ideal for high power density applications. The diode reverses recovery current is reduced, and the leakage inductance allows ZCS operation even in CCM. At ZVS, the switch turns on and off, and the voltage

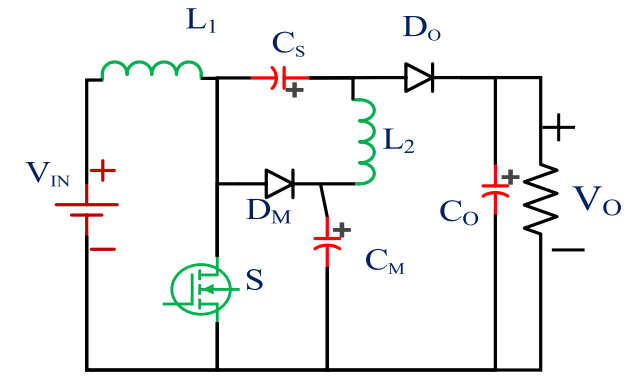

(a). Modified non-isolated SEPIC converter [98], [99]

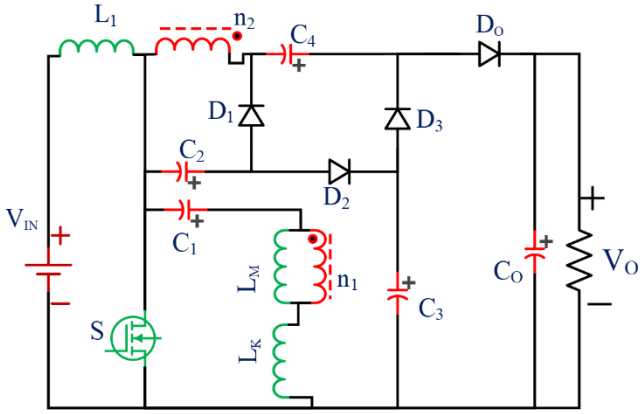

(b). Coupled inductor based modified SEPIC converter [100]

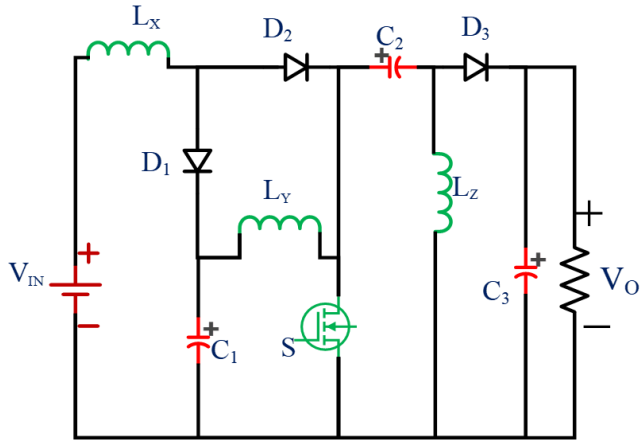

(c) . Modified SEPIC converter based hybrid SI and SC [101]

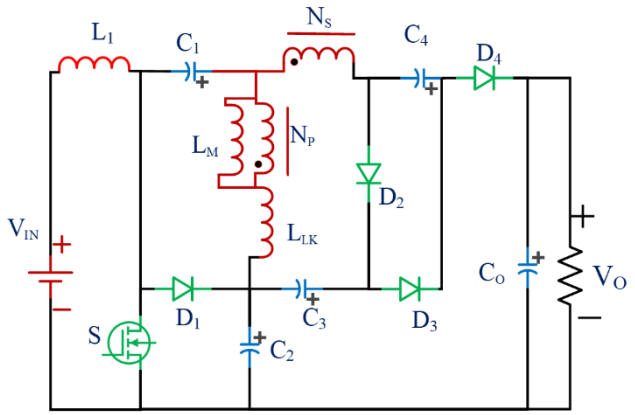

(d). Coupled inductor based hybrid SI and SC [102]

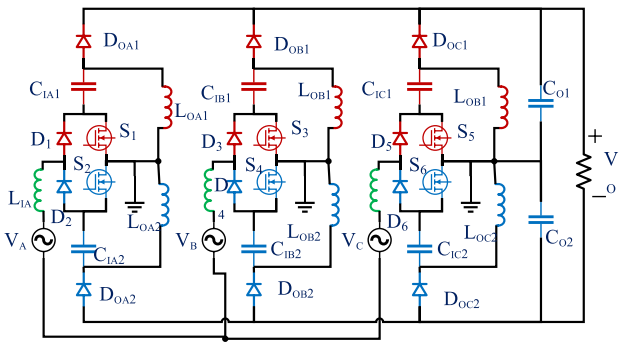

(e). AC-DC SEPIC converter based hybrid SC and SI for EV charging applications [103]

FIGURE 21. Hybrid switched capacitor and switched inductor-based SEPIC converters.

across the switch is half of the output voltage. Peak efficiency is stated to be 97% for 180W output power.

A single high-step-up switch DC-DC converter based on SEPIC converter is proposed in [106] as shown in Fig. 22. (c). The coupled inductor and voltage Tripler unit are responsible for high voltage gain. Quasi-resonant operation of leakage inductance of coupled inductors and capacitors reduces the switching losses. The suggested converter has significant drawbacks such as high input ripple current, voltage stress, switching losses, and reverse recovery voltage. The quasi-resonant operation decreases losses by reducing voltage stress on the power electronics switches. At the rated

TABLE 7. Review of sepic converter derived topologies' voltage gain and voltage stress expressions.

Reference	Gain	Voltage stress	Contributions
[89]	$V_s = V_D = V_o + \frac{3V_{in}}{4}$	NR	• Extended ZVS switching • Low switching loss • Hybrid control method • GaN switches – costly • Relatively less efficiency
[91]	$G = (n+1)(\frac{(D+D_b)}{D_d+D_r}+1)$ $D_d + D_r + D_\delta \le 1 - D$	$V_{DM1} = V_{CS1} + V_{L2P}; V_{DM2} = V_{CS2} + V_{L2S};$ $V_{DO} = V_O - V_{CM}$	• Usage of partially interleaved transformer • Planer components -compact • GaN switches and planner magnetic components -costly
[98], [99]	$G = \frac{2(D+D_b)}{D_d+D_r}+1$ $D_d + D_r + D_\delta \le 1 - D$	NR	• Integrated inductor to reduce power density • Reduced magnetic components losses
[106]	$G = \frac{1}{1-D}(2kn(1-Dk) + 1 + Dk + nDk^2$ $G_{ideal} = \frac{(n+1)D+1}{1-D} + 2n$	$V_{D0} = V_S = \frac{(n+1)V_o}{1+D+n(2-D)}$	• The voltage stress across the switches is rather considerable. • Ripple current is significantly notable
[100]	$G = \frac{2+n(1+D)}{1-D} + 2n$	$V_{Ds} = V_{D2} = V_{D1} = \frac{V_o}{2+n+nD};$ $V_{D3} = V_{D0} = \frac{(1+n)}{2+n+nD}V_o;$	• Used regenerative passive losses less passive circuit • No reverse recovery problems in Diodes
[101]	$G = \frac{D}{(1-D)^2}$	NR	• The new structure was developed • Simple circuit. • Continuous input current
[92]	$G_{CCM} = \frac{2n+1+D}{(1-D)}$ $G_{DCM} = \frac{(4n+3)+(D+D_B)-D_\delta}{1-(D+D_B)+D_\delta}$	$V_{S1,S2} = \frac{V_{IN}+V_O}{2(n+1)}; V_{DM1} = \frac{V_{IN}+V_O}{2(n+1)};$ $V_{DM2,DO} = \frac{n(V_{IN}+V_O)}{(n+1)};$	• Low voltage stress with high voltage gain • Although the converter operates in both CCM and DCM, integrating a switched inductor with a coupled inductor-based modified SEPIC converter • ZVS can only be performed in the discontinuous mode.
[90]	$G = \frac{3D+1}{1-D}$	$V_{DS.S1} = V_{DS.S2} = \frac{V_{IN}}{1-D};$ $V_{Da} = V_{DO} = \frac{2V_{IN}}{1-D};$	• The decreased voltage stress on the switches, as well as the noninverting output voltage, • Low conduction losses • Simple control • During the turn-off operation, there is no voltage overshoot for the switches.
[93]	$G = 1 + \frac{nD}{\frac{n-1}{1-D}V_{IN}}$	NR	• Wide control range • Easy operation • Less complex
[96]	$G = \frac{3D}{1-D}$	NR	• More number so devices used • Low switching stress for the switches.
[104]	$G = \frac{2+(2-D)N_{21}-(1+D)N_{31}}{(1-D)(1-N_{31})}$	$V_S = V_{DC} = \frac{(1-N_{31})V_{OUT}}{2+(2-D)N_{21}-(1+D)N_{31}}$ $V_{D1} = \frac{2+N_{21}-(1+D)N_{31}}{2+(2-D)N_{21}-(1+D)N_{31}}V_{OUT}$ $V_{D2} = V_{D0} = \frac{1+N_{21}-N_{31}}{2+(2-D)N_{21}-(1+D)N_{31}}V_{OUT}$	• A three-winding build in transformer is utilized for higher voltage gains • Low sized core

TABLE 7. *(Continued.)* **Review of sepic converter derived topologies' voltage gain and voltage stress expressions.**

[94]	$G = \frac{1+n}{(1-D)}$	$V_S = \frac{V_{IN}}{(1-D)}$; $V_{D1} = V_{D3} = \frac{nV_{IN}}{(1-D)}$ $V_{D2} = \frac{(1+n)V_{IN}}{(1-D)}$;	• Lower component count • Higher power density • Voltage Gain up to 10
[95]	$G = \frac{n_2 D}{(1-D)}$	NR	• Used Loss less snubber circuit • Highly efficient
[97]	$G = \sqrt{\frac{D^2 R_O}{4L_{eq} f_S}}$	$V_S = V_D = \frac{V_O}{4} + V_{IN}$; $V_{nS} = V_{nD} = \frac{V_O}{2+n} + V_{IN}$;	• Relatively complex • Operating in fixed duty cycle and reduced losses
[105]	$G = \frac{1}{(1+D)}$	NR	• High efficiency • How power density • No load limited • No high static gain technologies used
[102]	$G = 2 + n + \frac{D(n+1)}{1-D}$	$V_S = \frac{G+n+1}{2n+1} V_{IN}$; $V_D = 2 + n + \frac{D(n+1)}{1-D}$	• Higher power density • Low duty cycle • Losses due to switching are high
[103]	$G = \frac{D}{2}\sqrt{\frac{3R_0(L_a + L_{oa1})}{L_a L_{oa1} f_s}}$	NR	• The need for current control is eliminated • Low duty cycle • The gate driver's complexity

*G- gain; N- number of voltage levels; D-Duty ratio; k- coupling coefficient; V_{in}= input voltage V_0- output voltage; V_S - voltage stress across the switch; V_D-voltage stress across diode; NR- Not Reported.

100W output power, the output voltage achieved for an input voltage of 18V is 250V. The reported efficiency of the converter is 97.4% at the switching frequency of 40kHz.

Table 7 shows the gain and voltage stress between the switch and diode of several SEPIC converter topologies.

Table 8 analyses several SEPIC converter topologies based on component count, input voltage, output voltage, voltage gain, switching frequency, peak efficiency at rated power, cost, and complexity. The comparison assists us in determining the most cost-effective, less complicated, and efficient converter topology for sustainable EV charging applications.

F. INFERENCES

Without using magnetic components, switched capacitor circuits may deliver large power densities. A switched capacitor and inductor both charge and discharge in parallel. There should not be any magnetic element core saturation. The coupled inductor is more suitable for high voltage applications with fewer power losses. The snubber circuit minimises the voltage stress on the switch to a minimum. To achieve optimal efficiency, a low-voltage component with less parasitic features was used. By wrapping the inductors on a single core, core losses of the inductor and coupled inductor will also be decreased. The non-isolated converter is more compact and effective for high power applications. Quasi-resonant circuits provide high voltage gain and minimal voltage stress over power electronics switches.

VI. MODIFIED/ENHANCED CUK CONVERTER BASED TOPOLOGIES

The classical Cuk converter is capable of converting low-voltage input to high voltage output at an extreme duty ratio. Therefore, it introduces high current and voltage stress on the switching devices, thereby the efficiency of the converter is reduced. The Cuk converter fails to provide common ground between load and source due to its reverse polarity nature though it provides continuous input current and high efficiency in a lower duty ratio. Non-pulsating output and input currents with low Electromagnetic Interference (EMI) are the merits of the Cuk converter. Fig. 23 shows the classifications of Cuk converter derived topologies.

A. CUK+ LUO CONVERTER

For high gain applications, a transformerless Cuk converter is used with a positive super lift Luo converter is proposed in [107] and is illustrated in Fig. 24. This converter's major advantages include continuous input current, normalized voltage stress on the switches, size reduction of energy storage devices, common ground, and high gain with high efficiency. The Cuk converter provides continuous input current and high efficiency in a low duty ratio but fails to provide common ground to the load and source due to its reverse polarity nature. This shortcoming can be matched by integrating the Luo converter. The experimental validation of the converter was carried out with an input voltage of 40V, and the output voltage obtained is 120V.

TABLE 8. Sepic converter derived topologies- comparison based on the component count, input voltage output voltage, gain, efficiency at peak load.

Reference(s)	Element's count	T	Input voltage	Output voltage	Gain reported with switching frequency	Peak η at Reported Power	Cost ($)	complexity
[89]	L-3; C-3; S-2; D-2	10	12	12	G=10 at Fs=1MHz D = 0.5%	91.8% at 36W	87.6	**
[91]	L-1; C-5; S-1; D-4	11	24	200	G=8.33 at Fs=1MHz	93.1% at 80W	67.2	**
[98]	L-1; C-4; S-1; D-2	8	24	120	G=5 at Fs=1MHz D = 0.45%	91.5% at 36W	58.8	**
[106]	L-1; C-5; S-1; D-4	11	18	250	G=13.89 at Fs=40KHz D = 0.55%	96.6% at 100W	67.2	***
[100]	L-1; C-5; S-1; D-4	11	20	200	G=10 at Fs=60KHz D = 0.55%	97.3% at 100W	67.2	**
[101]	L-1; C-3; S-1; D-3	8	24	172	G=7.17 at Fs=50KHz D = 0.7%	91.4% at 100W	54	*
[92]	L-2; C-4; S-2; D-3	11	12	180	G=15 at Fs=500KHz D = 0.445-0.615%	93.4% at 54W	86.4	***
[90]	L-3; C-3; S-2; D-2	10	20	250	G=12.5 at Fs=40KHz D = 0.742%	93% at 200W	87.6	**
[93]	L-3; C-3; S-1; D-2	9	48	400	G=8.34 at Fs=100KHz D = 0.62%	94% at 400W	69.6	**
[96]	L-4; C-6; S-1; D-3	14	25	110	G=4.4 at Fs=33KHz D = 0.6%	93.3% at 110W	97.2	**
[104]	L-1; C-5; S-1; D-4	11	20	250	G=12.5 at Fs=55KHz D = 0.55%	94.4% at 200W	67.2	***
[94]	L-1; C-3; S-1; D-2	7	40	400	G=10 at Fs=100kHz D = 0.5%	95.2% at 400W	52.8	*
[95]	L-1; C-3; S-1; D-2	7	48	200	G=4.17 at Fs=50kHz D = 0.41%	93.8% at 100W	52.8	**
[97]	L-3; C-8; S-2; D-12	25	220	800	G=3.64 at Fs=50kHz D = 0.35%	93.9% at 1000W	129.6	****
[105]	L-1; C-3; S-2; D-1	7	30	200	G=6.67 at Fs=70kHz D = 0.73%	97% at 180W	69.6	**
[102]	L-2; C-5; S-1; D-4	12	20	300	G=15 at Fs=50kHz; D = 0.62%	93.5% at 245W	75.6	**
[103]	L-9; C-8; S-3; D-6	26	220	400	G=1.82 at Fs=50kHz; D = 0.35%	95.5% at 3000W	190.8	***

* L-No. of Inductors; C- No. of Capacitors; S- No. of switches; D- No. of Diodes; T-Total Components used; G-Gain; Fs-Switching Frequency; NR-Not Reported; *complexity level-low, ** complexity level-moderate; *** complexity level -high; **** complexity level-extra/ultra-high

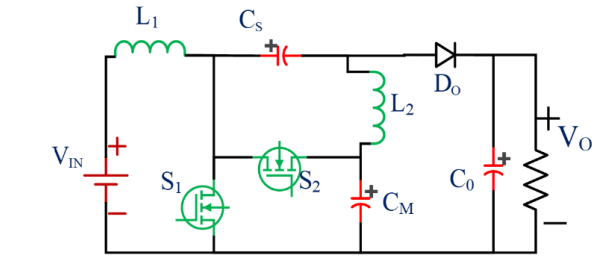

(a). Soft switched Modified SEPIC converter [104]

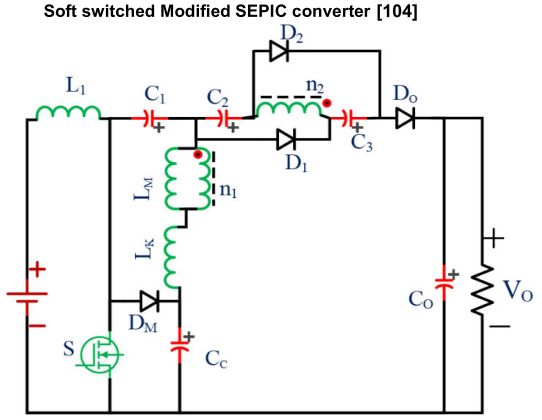

(b). ZCS based SEPIC Converter [105]

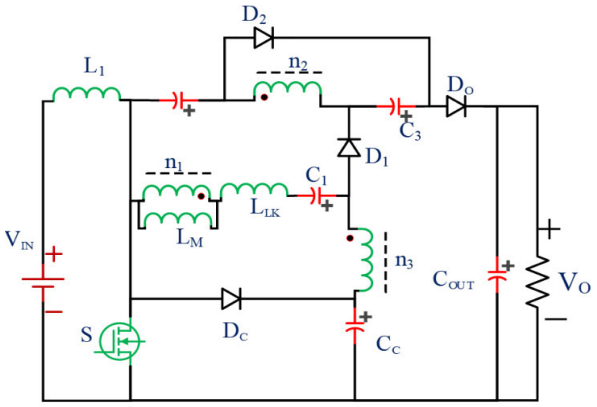

(c). Coupled inductor and voltage Tripler [106]

FIGURE 22. Quasi-resonance operation SEPIC converter.

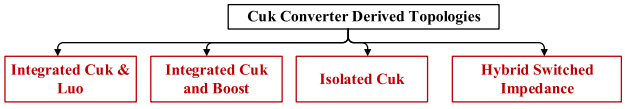

FIGURE 23. Classification of Cuk converter.

B. MERGED QUADRATIC BOOST AND CUK

Two non-isolated DC-DC high gain converters combine the advantages of quadratic boost and Cuk converters, such as high step-up voltage and easy control owing to shared ground [67]. Fig. 25. (a) shows the hybrid Quadratic boost converter 1 (HQBC type -1) and hybrid Quadratic boost converter 2 (HQBC type-2) shown in Fig. 25. (b). Multiphase converter reduces the current ripple and enhances the power handling capacity. The two topologies are termed hybrid Quadratic boost converter 1 (HQBC type-1) and HQBC type-2. A detailed study has been carried out to analyze these topologies' operation in both CCM and DCM modes. Experimental validation of both HQBC type-1 and HQBC type-2 was carried out with the output power of 250W and obtained 94.07% & 94.02% as the efficiencies respectively. The output voltage achieved for a 24V input voltage is 200V with a switching frequency of 20kHz and a duty ratio of 64%.

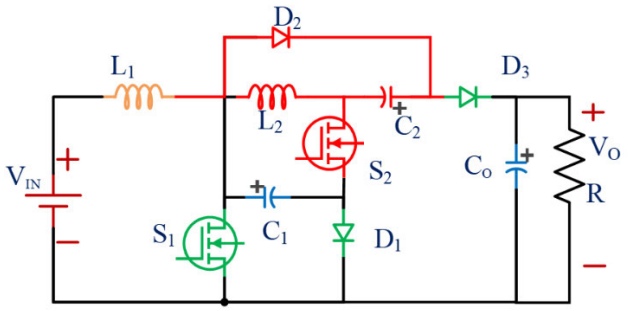

FIGURE 24. Transformerless high gain Cuk [107].

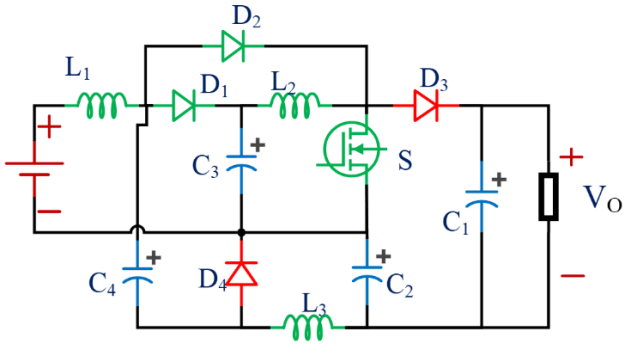

(a). HQBC converter type-I [67]

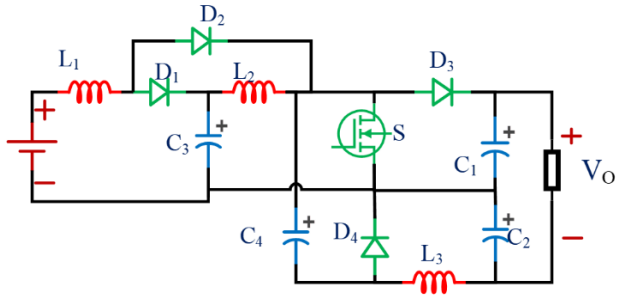

(b). HQBC converter type-II [67]

FIGURE 25. Quadratic DC-DC Boost-Cuk HQBC converter.

C. CUK CONVERTER BASED ON A HYBRID OF SWITCHED INDUCTOR (SI) AND SWITCHED CAPACITOR (SC)

Switched inductor (SI), switched capacitor (SC), voltage multipliers, and voltage lift converter topologies minimize voltage stress on semiconductor devices. To combine the

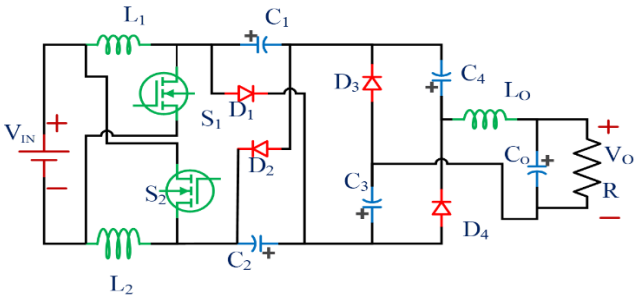

FIGURE 26. Active switched inductor Cuk converter [108].

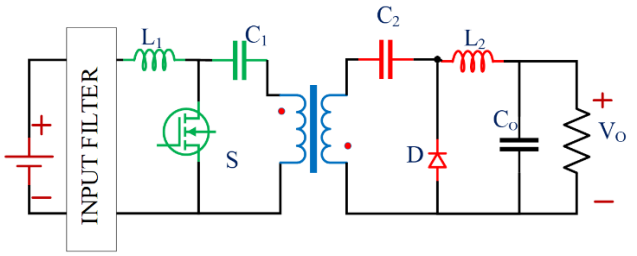

FIGURE 27. Isolated Cuk converter [109].

advantages of the switching inductor, capacitor, and Cuk converter, this article [108] proposed a Cuk converter with hybrid switched inductor and switched capacitor as shown in Fig. 26. The merits can be listed as

1) Output current that does not pulse.
2) The regulated and uncontrolled switches are subjected to low voltage stress.
3) Minimal current stress.
4) The operation is simple.
5) High voltage gain and efficiency.

The experimental efficiency of the converter reported is 97.86% for a 200W output power. With an input voltage of 37.4V, the output voltage is 400V at a switching frequency of 100kHz, and the duty ratio is 58.7 %. The total benefit obtained is 10.69.

D. ISOLATED CUK CONVERTER

The isolated Cuk converter with different filter topologies was applied and analyzed in [109]. Fig. 27 shows the isolated Cuk converter. The primary feature is the design of the state space average model of this converter with filters for its transfer function using small signal analysis. The SiC power switch is used to study the performance of the converter with filters. The efficiency reported is 86% at the output power of 50W.

Table 9 shows the gain and voltage stress across the switch and diode of various converter topologies covered in the section derived/enhanced/modified Cuk converter topologies.

Table 10 analyses several Cuk converter topologies based on component count, input voltage, output voltage, voltage gain, switching frequency, peak efficiency at rated power,

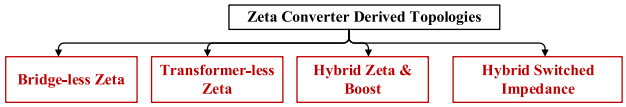

FIGURE 28. Classification of Zeta derived converter.

cost, and complexity. The comparison assists us in determining the most cost-effective, less complicated, and efficient converter architecture for sustainable EV charging applications.

E. INFERENCES

For converting low voltage input to high voltage output, the conventional Cuk converter offers a high duty ratio capacity. As a result, the switching devices are subjected to high current and voltage stress, which lowers the converter's efficiency. Due to its reverse polarity, the Cuk converter cannot establish a common ground between the load and the source, even if it offers continuous input current and high efficiency at a reduced duty ratio. High gain is supposed to have properties such as continuous input current, normalized voltage stress on the switches, size reduction for energy storage components, a common ground, and high gain with high efficiency. A simple control circuit should be employed. Voltage lift switches and switched inductors decrease voltage stress on semiconductor devices. Making use of the SiC power switch.

VII. MODIFIED/ENHANCED ZETA CONVERTER BASED TOPOLOGIES

Zeta converter can generate regulated output voltage above and below the input voltage as SEPIC converter. The merits of the Zeta converter over the SEPIC converter are lower output voltage ripple and simple compensation. Apart from the merits, the Zeta converter has a few demerits like high input voltage and a large flying capacitor. The classification of Zeta derived converter for EV charging is represented in Fig. 28.

A. HYBRID SWITCHED INDUCTOR AND SWITCHED CAPACITOR-BASED ZETA

A single switch Zeta converter for high voltage gain with low voltage stress, as shown in Fig. 29. (a). A single switch Zeta converter is proposed in [110] for high voltage gain with reduced voltage stress as presented in Fig. 29. (a). The assumptions made for analysis are 1) the capacitor's ripple voltage is negligible 2) all the devices are ideal. The proposed Zeta converter is studied in both CCM and DCM operations. The benefits of the proposed Zeta converter are as follows:

1) Since the converter employs a single switch, the drive and control are simple and cost-effective.
2) The number of fundamental cells varies depending on the application.
3) A low-duty cycle is used to produce the high voltage gain.

TABLE 9. Review of Cuk converter derived topologies' voltage gain and voltage stress expressions.

REFERENCE	GAIN	VOLTAGE STRESS	CONTRIBUTIONS
[107]	$G = \frac{2-D}{(1-D)^2}$	$V_{S1} = \frac{1}{1-D}V_{IN}; V_{S2} = \frac{1}{(1-D)^2}V_{IN};$ $V_{D1} = \frac{1}{1-D}V_{IN}$; $V_{D2} = \frac{1}{(1-D)^2}V_{IN};$ $V_{D3} = \frac{(2-D)}{(1-D)^2}V_{IN}$	• High step-up voltage gain with minimal voltage stress, non-pulsating output current • Current stress has been reduced across the component. • Simple to use
[67]	$G_{HQBC1} = \frac{1+D(1-D)}{(1-D)^2}$ $G_{HQBC1} = \frac{1+D}{(1-D)^2}$	NR	• Simple control • Conduction voltage drops in the active switch, diodes, and inductor parasitic resistors lead to deviation in the calculated values • Common ground
[59]	$V_0 = d_1V_{c1} + d_2V_{c2}$	NR	• Large input sources can be accommodated. • Because the output inductor is shared with the input ports, the number of components is reduced. • All ports have continuous current with low ripple. • Each input has its own power control.
[108]	$G = \frac{2D}{(1-D)}$ $V_S = V_D = \frac{1}{5-D}V_O$	NR	• Simple operation and control. • Continuous input current • Common ground • Reduced current stress across the component

*G- gain; N- number of voltage levels; D-Duty ratio; k- coupling coefficient; V_{in}= input voltage V_0- output voltage; V_S -voltage stress across the switch; V_D - voltage stress across the diode; and NR stands for Not Reported.

TABLE 10. Cuk converter derived topologies- comparison based on the component count, input voltage output voltage, gain, efficiency at peak load.

REFERENCE (S)	ELEMENT'S COUNT	T	INPUT VOLTAGE	OUTPUT VOLTAGE	GAIN REPORTED WITH SWITCHING FREQUENCY	PEAK η AT REPORTED POWER	COST ($)	COMPLEXITY
[107]	L-2; C-3; S-2; D-3	10	120	360	G=3 at Fs=45kHz	90% at 100W	80.4	***
[67]	L-3; C-4; S-1; D-4	12	24	200	G=8.34 at Fs=20kHz	94% at 250W	78	**
[59]	L-3; C-3; S-2; D-1	9	18-30	1	G=19at FS=20kHz	92.7% at 100W	75	**
[108]	L-3; C-5; S-2; D-4	14	37.4	400	G=10.7 at Fs=100kHz	97.86% at 200W	102	*
[109]	L-2+1; C-3; S-1; D-1	5	130	400	G=3.08 at Fs=42kHz	86% at 50W	85.2	***

* L-No. of Inductors; C- No. of Capacitors; S- No. of switches; D- No. of Diodes; T-Total Components used; G-Gain; Fs-Switching Frequency; NR-Not Reported; *complexity level-low, ** complexity level-moderate; *** complexity level -high; **** complexity level-extra/ultra-high

The highest experimental efficiency is 94.3 % for an output power of 240W with a voltage source of 48V and an output voltage of 240V with a duty cycle of 74%.

Based on the coat circuit, a bipolar high step-up Zeta buck-boost converter is proposed in [111]. The coat circuit is useful for reducing voltage stress and increased high gain. This

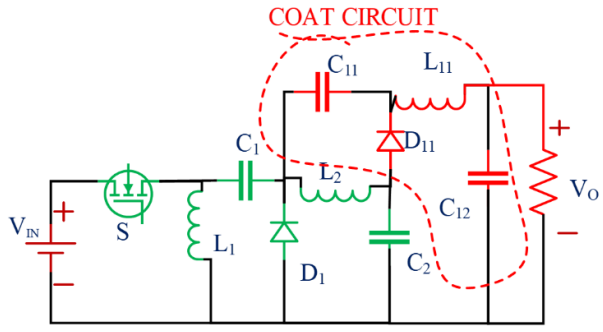

(a). Single switch Zeta converter [110]

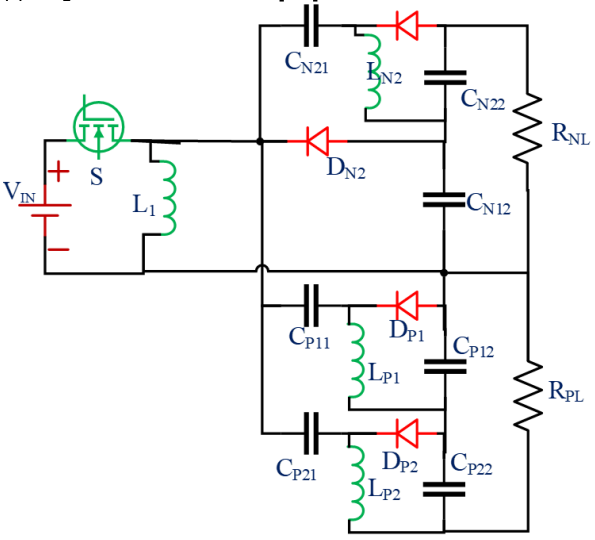

(b). Single switch Zeta converter for multi outputs [111]

FIGURE 29. Hybrid switched inductor and switched capacitor-based Zeta converter.

suggested design has a major advantage in that the positive and negative voltages of the converter's bipolar output voltage are automatically equalized. Fig. 29 (b) depicts a single switch Zeta Buck-Boost (ZBB) converter-based coat circuit. capable of high voltage gain and bipolar output. The assumptions listed for simplified analysis are:

1) All the elements are ideal, and all the parasitic effects are eliminated.
2) The capacitor ripple voltage effects are insignificant due to large capacitance.
3) CCM mode is used by the converter.

The benefits of the converter mentioned are:

1) Without any additional switch, drive, and control circuitry, this converter produces bipolar outputs.
2) The use of the Coat circuit reduces the voltage load on the switches.
3) According to the application requirements, the positive and negative cells can be extended.

B. HYBRID ZETA-BOOST CONVERTER + SWITCHED INDUCTOR

Hybrid Zeta and Active-quad-switched-inductor are proposed in [112] for high gain voltage as presented in

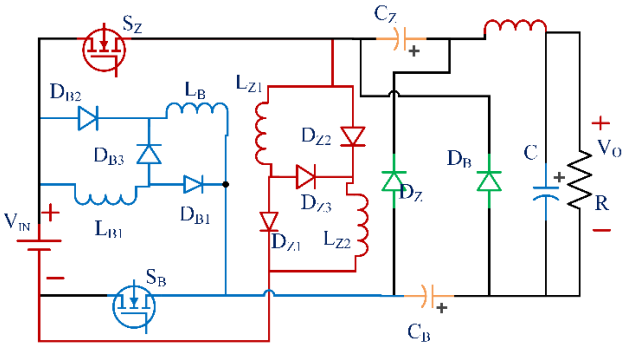

FIGURE 30. Hybrid Luo converter [112].

Fig. 30. High voltage gain is achieved with the use of high frequency transformers, multistage diodes, and capacitor circuits with continuous input and output currents. If the duty cycle of the converter is increased in order to achieve high voltage gain, the performance of the converter will decline. To counteract voltage spikes caused by isolated converters, a clamping circuit must be incorporated, reducing efficiency. The Luo converter can provide high voltage gain. However, complexity, volume, cost, and losses rise, while efficiency declines. The integrated Zeta active quad-switched inductor network has several features includes:

1) Excessive gain.
2) Input current that is constant.
3) Inductor with a low current rating.
4) Devices with low current/voltage ratings.

The experimental efficiency recorded is 92.93 % for a 500W output power and a 50V input voltage, resulting in a 400V output voltage.

C. TRANSFORMERLESS ZETA CONVERTER

A Transformerless Zeta converter configuration is proposed in [113] for high gain application as shown in Fig.31. The converter topology is very simple; because it employs a single adjustable switch, the complexity of the drive and control circuits is minimized. Both CCM and DCM modes may be used to study the converter. For the simplified analysis purpose, the assumptions made are:

1) Since all of the capacitors utilized are huge, the capacitor voltage is ripple free.
2) All the controlled and uncontrolled switches are ideal.

The Zeta converter presented has the below listed merits

1) Buck-boost ability
2) Continuous output current
3) The DC insulation between input and output is comparable to the various transformerless high gain topologies documented in the article's literature.

The claimed efficiency for the 200W output power is 96 %. At a switching frequency of 40kHz, the output voltage is 80V for a 36V input voltage.

TABLE 11. Review of Zeta converter-derived topologies' voltage gain and voltage stress expressions.

REFERENCE	GAIN	VOLTAGE STRESS	CONTRIBUTION
[110]	$G = \frac{2D}{(1-D)}$ (buck) $G = \frac{(n+1)D}{(1-D)}$ (boost)	$V_S = V_D = \frac{1}{(n+1)D} V_O$	• Simple control and drive circuits • Bipolar buck-boost converter
[111]	$G_P = \frac{mD}{(1-D)}$ (positive) $G_N = \frac{nD}{(1-D)}$ (negative)	NR	• Without the use of multiplier circuitry, voltage gain is high. • Input current is continuous, • Inductor with a low current rating, • Devices with low voltage/current ratings.
[112]	$G = \frac{1 + 5D + 2D^2}{(1 - D)}$	$V_S = \frac{1 + D}{(1 - D)}$ $V_D = \frac{2}{1 - D}$	• Low switching losses • Control is simple • simple topology
[113]	$G = \frac{2D}{(1 - D)}$	$V_S = V_D = \frac{1}{1 - D} V_{IN}$	• Reduced number of the output inductor • The controller is simple since it uses similar pulses
[114]	$G = \frac{N_2 D}{N_1 (1 - D)}$	NR	• Low switching losses • Low current rating inductor,

*G- gain; N- number of voltage levels; D-Duty ratio; k- coupling coefficient; V_{in}= input voltage V_0- output voltage; V_S - voltage stress across the switch; V_D-voltage stress across diode; NR- Not Reported

TABLE 12. Zeta converter derived topologies- comparison based on the component count, input voltage output voltage, gain, efficiency at peak load.

REFERENCE (S)	ELEMENT'S COUNT	T	INPUT VOLTAGE (V)	OUTPUT VOLTAGE (V)	GAIN REPORTED WITH SWITCHING FREQUENCY	PEAK η AT REPORTED POWER	COST ($)	COMPLEXITY
[110]	L-4; C-6; S-1; D-3	14	48	400	G=8.34 at Fs=100kHz	94.2% at 300W	97.2	**
[112]	L-5; C-3; S-2; D-8	18	50	400	G=8 at Fs=50kHz	92.93% at 500W	111.6	****
[113]	L-3; C-4; S-1; D-2	10	36	80	G=2.23 at Fs=40kHz	97% at 200W	75.6	**
[111]	L-M+n; C-2(m+n)-1; S-1; D-M+n	1	48	200	G=4.17 at Fs=100kHz	95.1% at 400W	102	***
[114]	L-1; C-3; S-2; D-4	10	12	48	G=4 at Fs=NR	NR at 1000W	69.6	**

* L-No. of Inductors; C- No. of Capacitors; S- No. of switches; D- No. of Diodes; T-Total Components used; G-Gain; Fs-Switching Frequency; NR-Not Reported; *complexity level-low, ** complexity level-moderate; *** complexity level -high; **** complexity level-extra/ultra-high

D. BRIDGELESS ISOLATED ZETA + LUO CONVERTER

Reference [114] proposes a Bridgeless (BL) isolated Zeta-Luo converter for power factor control on the supply side for EV charging applications illustrated in Fig.32. The single inductor shared by two converters for both cycles improves efficiency. For all operating conditions, the measured power quality is within the limitations established by the suggested IEC 61000-3-2 norm. The Zeta and Luo converter offers extraordinary improvement in power quality, load regulation and low charging current ripple. The substantial features of the proposed charger configuration are:

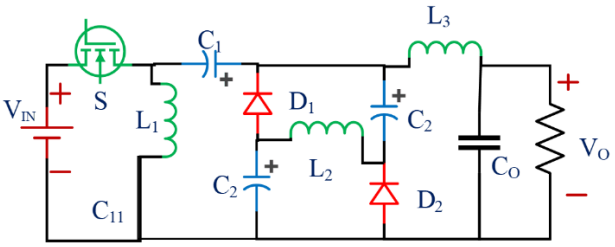

FIGURE 31. Non-isolated buck-boost converter Based on Zeta converter [113].

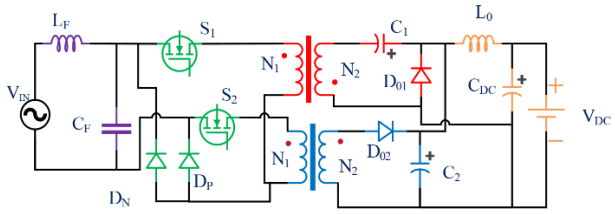

FIGURE 32. Bridgeless (BL) isolated Zeta–Luo converter based EV charger [114].

1) The reduction in the overall size of the converter is due to the sharing of a single inductor at the output of Zeta and Luo converters.
2) Efficiency is improved due to the reduction of components.
3) Converter operates in DC mode due to magnetizing inductor in the isolated converter.
4) A simplified simultaneous pulse has perfect control over the power factor.

Table 11 presents the gain and voltage stress across the switch and diode of various converter topologies discussed under derived/enhanced/modified Zeta converter topologies.

Table 12 compares various ZETA converter topologies based on the component count, input voltage, output voltage, voltage gain, switching frequency, and peak efficiency at the rated power, cost, and complexity level. The comparison helps us to find the cost-efficient, less complex more efficient converter topology that suits sustainable EV charging applications.

E. INFERENCE

The converter's closed-loop control is utilized to comprehend the dynamic behavior of the converters. The high frequency transformer and multistage diode and capacitor circuits offer significant voltage gain. A clamping circuit must be added to avoid voltage spikes produced by non-isolated converters, which will decrease efficiency. If the high gain output voltage is reached by raising the duty cycle of the converter, the converter's performance will suffer. The drive and control circuits' complexity will be reduced. The CCM and DCM modes can both be used to investigate the converter's performance. The power quality obtained is within the limitations given by the required IEC 61000-3-2 standard for all operating conditions.

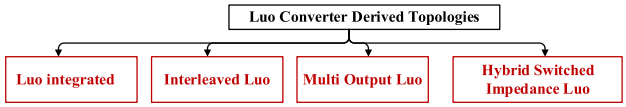

FIGURE 33. Classification of Luo converter derived topologies.

VIII. MODIFIED/ENHANCED LUO CONVERTER BASED TOPOLOGIES

At a low duty cycle, the Luo converter may give high gain and good efficiency. When compared to boost converters, Luo converters have a higher conversion ratio, higher power density, more efficiency, and a more inexpensive construction [115]. However, this converter's drawback is a relatively low output current, which renders the Luo converter ineffective. It is combined with a buck converter to enhance performance. As a result, the Luo-buck integrated topology will enhance the crucial factors that make the traditional Luo converter effective. To make the Luo converter suitable for the EV charging application, literature reports various modifications listed as shown in Fig. 33.

A. LUO INTEGRATED CONVERTERS

A Multiport Converter integrated buck and Super lift Luo converter is proposed in [116] as shown in Fig. 34. (a). The electric motor, audio system, and light all operate at different voltage levels in the EV. The SLBC (super lift with buck converter) produces two step-up voltages and one step-down voltage. The duty cycle of the switches D1 varies from 60-80% for the fixed D2=50%. The various combinations of the duty cycle were analyzed. The gain for step up is 6 and 2.3 for step down. For a 150W output power, the experimental efficiency is 93 %. The step-up and step-down output voltages for a 12V input are 25V and 5.2V, respectively. The essential characteristics include ease of control, a wide voltage range with enhanced gain, and reduced conduction loss.

The bridgeless modified Luo converter is presented in [117] to provide vigorous charging action across a wide input voltage range, as illustrated in Fig. 34. (b). The main goals of the article are:

1) Removal of input diode.
2) Less number of components operating in a single switching cycle.
3) The input filter is not required because of the input inductor of the modified Luo converter.
4) Both switches use the same gate pulse, which makes control simple.
5) The output inductance provides continuous current though the converter is operating in DCM.
6) Conduction losses are reduced.

The experimental validation is configured to charge 48V/100Ah with an output power of 850W. The DC link voltage is 300V, and the switching frequency is 20kHz.

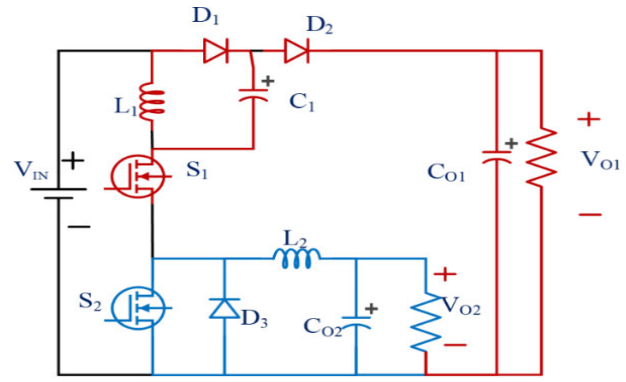

(a). Integrated Super lift Luo and buck converters [116]

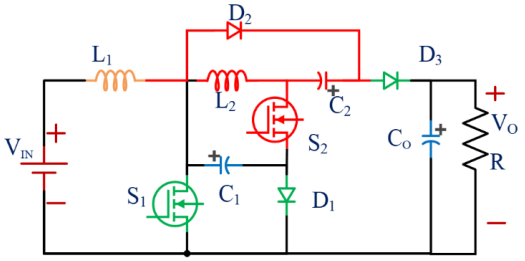

(b). Bridgeless modified Luo converter [117]

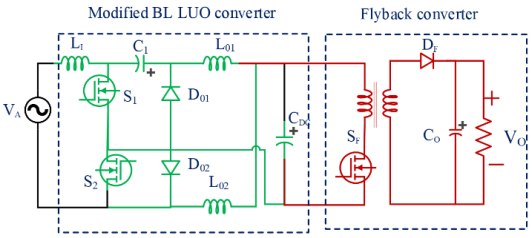

(c). Integrated Luo and flyback converters [107]

FIGURE 34. Luo integrated converters.

Cuk with a positive output super lift Luo converter for a transformerless high gain is proposed in [107] as shown in Fig. 34. (c). This converter's characteristics include constant input current, low voltage/current stress, decreased size of energy storage parts, common ground, high gain, and high efficiency. The Luo converter can provide high gain with high efficiency at a low duty cycle. The voltage lift is used for obtaining high gain at a reduced component count. The capacitor voltage (VC1) of the Cuk converter is similar to the capacitor voltage of a typical boost converter. The two switches operate simultaneously hence, the control complexity of employing two switches is reduced. The theoretical efficiency is more than 80%. The switch's duty cycle is 67 %. At a rated power of 200W, the input voltage is 20V and the output voltage is 120V. The switching frequency of the converter is 100kHz.

B. INTERLEAVED LUO CONVERTER

A New interleaved Luo converter is proposed [118] for a pre-regulated power factor built for EV battery

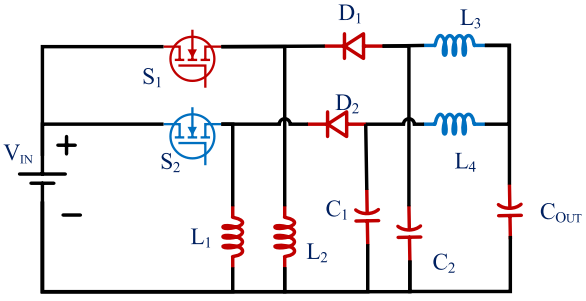

FIGURE 35. Interleaved Luo converter [118].

charging. Fig. 35 shows the interleaved Luo converter for the pre-regulated power factor. Interleaving two Luo converters helps in effective charging at high power. The reduction in the switch's current stress reduces conduction loss. Hence, efficiency is increased. The converter operates in DCM for the zero switching of the switch and the improvement of the reverse recovery of the diode. The high power rating and voltage lifting features of this Luo converter make it appropriate for an improved power factor-based EV charger. The input current of the two-phase interleaved Luo converter is continuous with lower input current, and the battery life is extended.

The commendable features of this Luo converter are

1) Since the Luo converter interleaves, the input current is split, reducing the switch's current stress.
2) Reduced current stress allows for the use of low-rated switches, which decreases the cost, size, and efficiency of the converter.
3) Interleaving reduces the input current ripple.
4) Due to the low output ripple, the size of the DC link capacitor was also lowered.

For the rated output power of 750W, the converter's experimental efficiency is 91.89 %. The input voltage is 220V, the supply frequency is 50Hz, and the output voltage is 300V.

C. MULTI-OUTPUT LUO CONVERTER

Super lift Luo converter, flyback, and coupled inductor-based enhanced multi-output converter integrated is presented in [119] as shown in Fig. 36. To achieve great efficiency, the coupled inductor's leakage inductance is regenerated. As a result, the voltage spike caused by leakage inductance is handled, and it will no longer arise across switches. The positive output super lift Luo converter has remarkable advantages such as high efficiency, superior power density, and high gain. As the inductors are wound on the same core, the size of the converter is reduced.

For analysis the following assumption was made:1) converter operates in CCM 2) the forward voltage drop of the diode is equaled to the resistance drop and coupled inductor and capacitor effects are eliminated. The connected inductor has no effect on the voltage stress across the switches. The voltage stress on the switch, on the other hand, is fully

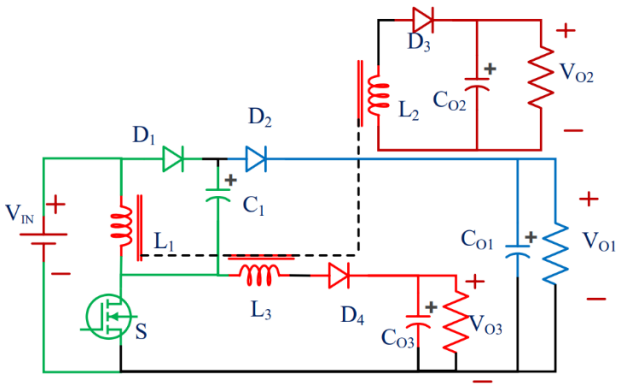

FIGURE 36. Multi-Output Luo converter [119].

determined by the duty cycle and input supply. The experimental model was developed for 110W output power, and the reported efficiency is 92.5%. For the input voltage of 12V, multiple output voltages obtained are 48V,36V, and 24V at the switching frequency of 115kHz.

D. SWITCHED IMPEDANCE BASED LUO CONVERTER

Modified Luo converter for EV charging system to provide high voltage gain, low voltage stress on switches, decreased capacitor stress, and reduced component count is proposed in [120] as shown in Fig. 37. (a). The substantial challenge faced while integrating sources like batteries and supercapacitors with traction motors is inevitable. The article's significant contributions include:

1) The capacitor voltage stress of the modified Luo converter is reduced.
2) The failure of the capacitor depends on the voltage stress of the capacitor.
3) Cascading for high gain, high power applications.

Fig. 37. (b) shows the type-1 Switched Impedance based Luo converters and Fig. 37. (c) shows the type-2 Switched Impedance based Luo converters. AC -DC isolated bridgeless (BL) positive Luo converter for light vehicle applications is proposed in [121]. The main contributions are:

Simple, cost-effective, and reliable charging solution for light electric vehicle applications.

Positive output Luo voltage polarity utilizes minimum devices.

Enables soft switching, size reduction, high frequency discontinuous inductor current mode (DICM)

The prototype model was tested at various testable conditions.

The suggested converter has a laboratory efficiency of 91 % for a rated output power of 150W. For the input of 220V, 50Hz single phase supply obtained output voltage level is 85-265V while the switching frequency is 20kHz. The 24 V battery is taken as a load for laboratory validation.

Table 13 presents the gain and voltage stress across the switch and diode of various converter topologies discussed under derived/enhanced/modified Luo converter topologies.

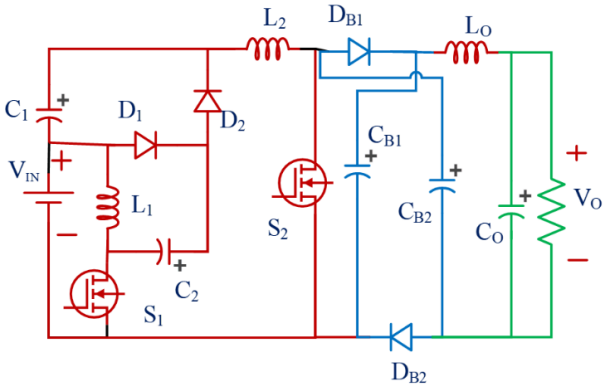

(a) Modified Luo converter for EV charging system [131]

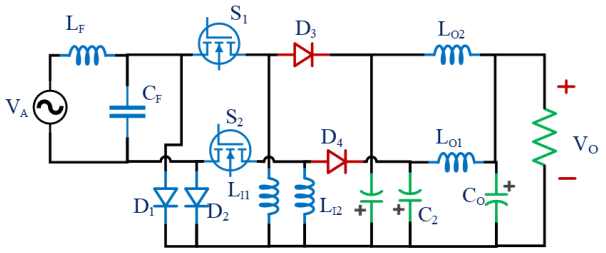

(b) Switched Impedance based Luo converters type-1 [130]

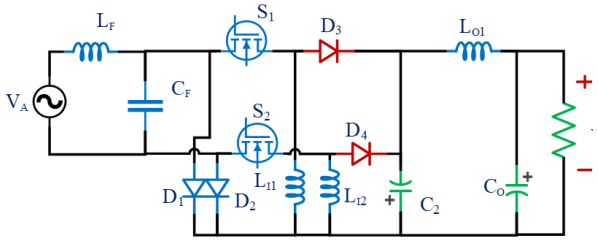

(c) Switched Impedance based Luo converters type-2 [130]

FIGURE 37. Switched impedance based Luo converter.

Table 14 compares various Luo converter topologies based on the component count, input voltage, output voltage, voltage gain, switching frequency, and peak efficiency at the rated power, cost, and complexity level. The comparison helps us to find the cost-efficient, less complex, more efficient converter topology that suits sustainable EV charging applications.

E. INFERENCE

It is expected that the integration of power sources like batteries and supercapacitors with traction motors will have significant challenges. Simple, affordable, and reliable charging solution for applications involving light electric vehicles provided by a modified Luo converter. To achieve great efficiency, the coupled inductor's leakage inductance is recycled. As a result, the voltage spike generated by leakage inductance is managed and will not occur across switches. The coupled inductor's leakage inductance is recycled to attain high efficiency. The voltage spike induced by leaking inductance is dealt with and will not arise across switches. It is

TABLE 13. Review of Luo converter-derived topologies' voltage gain and voltage stress expressions.

REFERENCE	GAIN	VOLTAGE STRESS	CONTRIBUTIONS
[116]	$G_1 = \frac{2 - D_2}{1 - D_2}$		• Lower input and output current ripples • Simplicity in control • Current flows through less number of components over one switching interval • Reduction in conduction loss
[120]	$G_{EVEN} = \frac{(2 - D)[(M + 1) - D]}{(1 - D)^2}$ $G_{ODD} = \frac{(2 - D)(M + 1)}{(1 - D)^2}$	$V_{S1} = \frac{V_{IN}}{1 - D}$ $V_{S2} = \frac{(2 - D)V_{IN}}{(1 - D)^2}$	• Low switch stress and turn-on capacitive losses • The three-coupled inductor uses a single core. • Simple and cost-effective
[119]	$G_1 = \frac{2-D}{1-D}; G_2 = \frac{DN_B}{1-D};$ $G_3 = \frac{1+\frac{D}{N_A}}{1-D};$	NR	• Simple architecture, • Least cost • Minimal capacitor stress • Improved controllability • Very low-duty cycle
[107]	$G = \frac{(2-D)}{(1-D)^2};$ $G_{DCM} = \frac{D+D_1}{{D_1}^2};$	$V_{S1} = V_{D1} = \frac{V_{IN}}{(1-D)};$ $V_{S2} = V_{D2} = \frac{V_{IN}}{(1-D)^2};$ $V_{D3} = \frac{(2-D)V_{IN}}{(1-D)^2};$	• Continuous output current; • The switches and diodes are subjected to low voltage strains. • Low current stress throughout the components • Operational simplicity; • Voltage gain and efficiency are both high.

*G- Gain; N- Number of Voltage Levels; D-Duty Ratio; k- Coupling Coefficient; V_{in}= Input Voltage V_0- Output Voltage; V_S - Voltage Stress across the Switch; V_D-Voltage Stress in a Diode

TABLE 14. Luo converter derived topologies- comparison based on the component count, input voltage output voltage, gain, efficiency at peak load.

Reference (s)	ELEMENT'S COUNT	T	INPUT VOLTAGE (V)	OUTPUT VOLTAGE (V)	GAIN REPORTED WITH SWITCHING FREQUENCY	PEAK η AT REPORTED POWER	COST ($)	COMPLEXITY
[119]	L-1; C-4; S-1; D-4	10	12	48	G=4 at Fs=115kHz D = 66%	NR% at 110W	61.2	**
[118]	L-4; C-3; S-2; D-2	11	220	300	G=1.37 at Fs=20kHz D = 40%	91.89% at 750W	96	***
[120]	L-3; C-5; S-2; D-4	14	12	108	G=9 at Fs=50kHz D = 25%	NR % at 50W	102	*
[116]	L-2; C-3; S-2; D-3	10	12	25	G=2 at Fs=NR D = D1=30 D2=60%	98.5% at 150W	80.4	***
[107]	L-2; C-3; S-2; D-3	10	20	120	G=6 at Fs=100kHz D = 67%	>80% at 200W	88.8	***

* L-No. of Inductors; C- No. of Capacitors; S- No. of switches; D- No. of Diodes; T-Total Components used; G-Gain; Fs-Switching Frequency; NR-Not Reported; *complexity level-low, ** complexity level-moderate; *** complexity level -high; **** complexity level-extra/ultra-high

expected that the integration of power sources like batteries and supercapacitors with traction motors will have significant challenges. Simple, affordable, and reliable charging solution for applications involving light electric vehicles provided by a modified Luo converter. To achieve great efficiency, the coupled inductor's leakage inductance is recycled. The voltage spike caused by leakage inductance is handled, and it won't appear across switches. The converter's size has decreased

TABLE 15. Effective converters for dc fast charging in practical on large scale.

Reference (s)	Element's count	T	Input voltage	Output voltage	Gain reported with switching frequency	Peak η at Reported Power	cost ($)	complexity
[72]	L-2; C-2; S-1; D-3	8	40	250	G=6.25 at Fs=50kHz	NR at 200W	87.6	**
[105]	L-1; C-3; S-2; D-1	7	30	200	G=6.67 at Fs=70kHz;	97% at 180W	69.6	**
[59]	L-3; C-3; S-2; D-1	9	18-30	18-30	G=19 at FS=20kHz	92.7% at 100W	75	**
[106]	L-1; C-5; S-1; D-4	11	18	250	G=13.89 at Fs=40KHz;	96.6% at 100W	67.2	***
[110]	L-4; C-6; S-1; D-3	14	48	400	G=8.34 at Fs=100kHz	94.2% at 300W	97.2	**

* L-No. of Inductors; C- No. of Capacitors; S- No. of switches; D- No. of Diodes; T-Total Components used; G-Gain; Fs-Switching Frequency; NR-Not Reported; *complexity level-low, ** complexity level-moderate; *** complexity level -high; **** complexity level-extra/ultra-high

since the inductors are coiled on the same core. The voltage stress at the switches is unaffected by the associated inductor.

However, the duty cycle and input supply have no effect on the voltage stress on the switch. The switch's current stress is lowered, minimizing conduction loss and enhancing efficiency. The converter increases diode reverse recovery by operating in DCM for switch zero switching. This Luo converter is suitable for enhanced power factor based EV chargers because of its high power rating and voltage boosting capabilities. The characteristics of this converter include a steady input current, low voltage/current stress, smaller energy storage parts, common ground, high gain, and high efficiency. The Luo converter has a high gain, high efficiency, and low duty cycle capability. Using the voltage lift makes it possible to get a high gain with fewer components.

Various high gain converter topologies were studied in this article, and the majority of the converters were considered to be suitable for EV DC charging applications. A converter may be selected depending on EV system requirements such as voltage gain, efficiency, ripples, and compatibility. A discussion on the mentioned dc-dc converters for EV-sustainable dc-dc fast charging applications, the aforementioned selection factors and the corresponding converters have been presented as follows. The component count comparison is the primary and simple approach to analyzing the suitability of the converter for any application. To attain high voltage gain, the increased use of diodes, switched inductors [77], [82], [83], [108], [112], switched capacitors [77], [82], [83], [97], [108], output rectifiers, stacked structures, integrated cells [10], [98], and clamp circuits [122] is unavoidable. Passive components, particularly magnetic cores, are the most effective means of measuring the volume and weight of the converter. The use of multi-winding magnetics [73], [75], [86], [87], [93] like a coupled inductor, conventional transformer, and built-in transformer helps in increasing the voltage gain. Furthermore, increasing the degree of freedom of the converter results in high efficiency if the parasitic inductance is recycled. The Magnetic coupling-based converters find a wide range of applications in EV fast charging applications, renewable energy systems and microgrids [9], [10], [17], [47], [68], [88]. Furthermore, these converters are used in data centres, telecommunications, physics, and high-power supply.

Multistage is also known as cascading [75], [78], [79], [86], [119]. It is developed by connecting the identical or different high step-up converters serially. The problem of lower efficiency due to converter multiplication can be solved by driving the low voltage stage at a high frequency and the high voltage side at a low frequency. The main challenges of the non-isolated high gain converters are high input current and its high ripple, making the input components design complex and increasing the size. To overcome these concerns, interleaving [73], [79], [91], [118] is recommended by connecting two or more identical converters in parallel at the input and extending this till the output port. Interleaving helps:

(1) to reduce the diodes' reverse recovery
(2) to increase power density
(3) in enhancing the reliability of the converter
(4) in achieving the wide operation range
(5) to reduce passive component size.

Multilevel topologies require fewer magnetic components, which reduces weight and EMI. Multilevel topologies [78], [79], [86], [119] have been offered as a common and practical solution for high voltage stress on output port components while preserving high voltage gain.

In some works, SI and SC are incorporated to obtain higher gains. Switched inductor and switched capacitors are made

to charge in parallel and discharge in series [77], [82], [83], [97], [108] and SI [77], [82], [83], [108], [112]. The essential aspects of SI and SC structures are outlined below.

(1) Requirement of magnetic inductors is eliminated since switched capacitor is used for power transmission. Hence, it is cheaper and reduced weight. EMI is also reduced.

(2) SCs have a less power density compared to the power density of SI. To reduce the switching losses and voltage spikes across the devices, switching frequency has to be high.

(3) The use of coupled inductors in SI networks [75], [77], [82], [83], [108], [112] improves voltage gain, reduces use of magnetic cores, makes simple with variable turns ratio of coupled inductor, the reverse recovery issue of diode is eliminated, provided the leakage inductance is recycled.

(4) The SI and SC circuits offer cascade, integration, and modularity capabilities, allowing them to achieve significant voltage gains.

(5) By adding a tiny resonant inductor to selected SC cells, the switching devices achieve zero current switching (ZCS) [21], [71], [79], [88], [92], [105], makes this suitable for operating at high power density and high switching frequency.

(6) the VMC are expected to be located after the main power switch, in order to minimize the voltage stress [73], [75], [79].

Despite their shortcomings, most non-isolated high gain DC-DC converters are appropriate for EV rapid charging applications [7], [64], [121].

To optimize an EV charging system, it is important to use a highly efficient converter that has high voltage gain, creates low semiconductor stress, and produces minimal voltage and current ripple. While high-order SC and SI cells can enhance voltage gain, they also increase the number of components. Some converters use snubbers and clamp circuits to reduce voltage stress, decrease switching loss, and improve efficiency and power density. Based on these considerations, the best converters for EV Sustainable DC Fast Charging Applications reviewed in this paper have been identified, one from each group, and presented in Table 15.

IX. RESEARCH OPPORTUNITIES

- Many Boost, SEPIC, Cuk, Luo, and Zeta derived converter topologies were developed and reported for high gain applications with various duty cycles ranging from 0.33 to 0.8. Efficiency suffers due to the significant conduction losses when the converter operates with a duty cycle of more than 0.5.
- Cascading converters develop quadratic and cubic converters. The gain achieved by the quadratic converter is higher than the conventional boost converter. However, voltage stress and high current are the major drawbacks.
- The quasi-resonant-based reduces switching losses and attains high gain. But it increases the complexity of the converter.

TABLE 16. Design considerations for the converters.

Design Considerations	Details
Size	Size, weight, power density, and energy density
Electrical performance	Power loss, electrical insulation, switching frequency, current rating, voltage rating, and EMI (Electromagnetic Interference)
Thermal management	Circulation of temperature, thermal Resistance, heat Capacity, and Thermal Expansion Coefficient
Mechanical strength	Vibration and Shock from outside
Reliability	Temperature Lifespan, and Power Cycling

- In the coupled inductor structure, the voltage and current stress of the switches are limited. Nevertheless, major problem with coupled inductor structures are loss due to the leakage. To address this issue, an additional clamping circuit to reuse the leakage energy is required but this again increases the complexity and controllability of the converter.
- Though the interleaving technique has reduced ripple current for high-power applications, the number of switches used is high compared to the gain achieved.
- Switched impedance like SC based topologies, capacitor charges in parallel, and discharges in series. Here, the voltage regulation is poor. Therefore, this methodology cannot be used individually. However, this can be integrated with other topologies which can have proper output voltage regulation.
- SI (switched inductor) based topologies charge parallelly and discharge serially the stored energy but the number of switches increases the cost, switching, and conduction losses.

Table 16 lists various consideration for designing the converters for EV DC fast charging applications which are size (reflects on the cost of the converter), electrical performance (ensure the requirement of the EV charging are met), thermal management (ensures the capability of the converter to withstand the temperature variation in and around the converter), mechanical strength (ensure the converter capability to withstand the external or internal shock and vibrations), reliability, manufacturability.

X. CONCLUSION

With superior wisdom of consciousness on environmental impacts due to fossil fuel and to reduce the dependency on conventional fuels reviewed the suitability of the DC-DC

converters interfacing the renewable/ sustainable sources for DC fast charging of EVs is attempted. In this article, the various standards and technical specifications of DC fast charging are presented along with the importance of power electronics in EV charging applications. the various topologies based on Boost, SEPIC, Cuk, Luo, and Zeta converters were discussed in detail with experimental parameters. Tabulated the expressions for the voltage gain and stress across controlled and uncontrolled switches with merits and limitations of the mentioned converter topologies were presented. A comparison table compares the total component count, input voltage, output voltage, power, and efficiency of the various topologies of Boost, Cuk, SEPIC, Zeta and Luo converters separately.

The existing topologies that face issues like high ripple input current, low impedance, voltage stress and current stress, leakage inductance, etc. were also discussed. The usage of coupled inductors introduces leakage inductance which requires active clamp circuits for attending the leakage inductance. The attempted leakage inductance increases the voltage stress across the switches and reverses the recovery problem in diodes. The primary objective of the converter should be significant gain along with excellent efficiency in a small size and weight. The increase in element count increases the loss therefore the efficiency can come down/ reduced, also size and weight increase.

REFERENCES

[1] I-Energy Agency. (2022). *Global EV Outlook 2022 Securing Supplies for an Electric Future*. [Online]. Available: https://www.iea.org/t&c/

[2] A. Ahmad, Z. Qin, T. Wijekoon, and P. Bauer, "An overview on medium voltage grid integration of ultra-fast charging stations: Current status and future trends," *IEEE Open J. Ind. Electron. Soc.*, vol. 3, pp. 420–447, 2022, doi: 10.1109/OJIES.2022.3179743.

[3] *International Review on Integration of Electric Vehicles Charging Infrastructure With Distribution Grid Report 2 Integration of Electric Vehicles Charging Infrastructure With Distribution Grid: Global Review, India's Gap Analyses and Way Forward in Cooperation With Led by IIT Bombay*, NDC Transp. Initiative Asia (NDC-TIA), Federal Ministry Environ., Nature Conservation, Nucl. Saf. Consumer Protection (BMUV), India, Aug. 2021.

[4] S. Deb, M. Pihlatie, and M. Al-Saadi, "Smart charging: A comprehensive review," *IEEE Access*, vol. 10, pp. 134690–134703, 2022, doi: 10.1109/ACCESS.2022.3227630.

[5] M. Loganathan, W. Issa, and S. Sheffield. (2021). *High Gain Power Converters For Electric Vehicles: A Review*. [Online]. Available: https://www.researchgate.net/publication/352957775

[6] J. A. Sanguesa, V. Torres-Sanz, P. Garrido, F. J. Martinez, and J. M. Marquez-Barja, "A review on electric vehicles: Technologies and challenges," *Smart Cities*, vol. 4, no. 1, pp. 372–404, Mar. 2021, doi: 10.3390/smartcities4010022.

[7] M. Safayatullah, M. T. Elrais, S. Ghosh, R. Rezaii, and I. Batarseh, "A comprehensive review of power converter topologies and control methods for electric vehicle fast charging applications," *IEEE Access*, vol. 10, pp. 40753–40793, 2022, doi: 10.1109/ACCESS.2022.3166935.

[8] G. Rajendran, C. A. Vaithilingam, N. Misron, K. Naidu, and M. R. Ahmed, "A comprehensive review on system architecture and international standards for electric vehicle charging stations," *J. Energy Storage*, vol. 42, Oct. 2021, Art. no. 103099, doi: 10.1016/j.est.2021.103099.

[9] D. S. Abraham, B. Chandrasekar, N. Rajamanickam, P. Vishnuram, V. Ramakrishnan, M. Bajaj, M. Piecha, V. Blazek, and L. Prokop, "Fuzzy-based efficient control of DC microgrid configuration for PV-energized EV charging station," *Energies*, vol. 16, no. 6, p. 2753, Mar. 2023, doi: 10.3390/en16062753.

[10] A. D. Savio, C. Balaji, D. kodandapani, K. Sathyasekar, R. Naryanmoorthi, C. Bharatiraja, and B. Twala, "DC microgrid integrated electric vehicle charging station scheduling optimization," *J. Appl. Sci. Eng.*, vol. 26, no. 2, pp. 253–260, 2023, doi: 10.6180/jase.202302_26(2).0011.

[11] H. Wang, A. Gaillard, and D. Hissel, "A review of DC/DC converter-based electrochemical impedance spectroscopy for fuel cell electric vehicles," *Renew. Energy*, vol. 141, pp. 124–138, Oct. 2019, doi: 10.1016/j.renene.2019.03.130.

[12] S. Hemavathi and A. Shinisha, "A study on trends and developments in electric vehicle charging technologies," *J. Energy Storage*, vol. 52, Aug. 2022, Art. no. 105013, doi: 10.1016/j.est.2022.105013.

[13] N. Daina, A. Sivakumar, and J. W. Polak, "Electric vehicle charging choices: Modelling and implications for smart charging services," *Transp. Res. C, Emerg. Technol.*, vol. 81, pp. 36–56, Aug. 2017, doi: 10.1016/j.trc.2017.05.006.

[14] L. Rubino, C. Capasso, and O. Veneri, "Review on plug-in electric vehicle charging architectures integrated with distributed energy sources for sustainable mobility," *Appl. Energy*, vol. 207, pp. 438–464, Dec. 2017, doi: 10.1016/j.apenergy.2017.06.097.

[15] J. Shi, M. Tian, S. Han, T.-Y. Wu, and Y. Tang, "Electric vehicle battery remaining charging time estimation considering charging accuracy and charging profile prediction," *J. Energy Storage*, vol. 49, May 2022, Art. no. 104132, doi: 10.1016/j.est.2022.104132.

[16] S. S. Ravi and M. Aziz, "Utilization of electric vehicles for vehicle-to-grid services: Progress and perspectives," *Energies*, vol. 15, no. 2, p. 589, Jan. 2022, doi: 10.3390/en15020589.

[17] S. Bracco, F. Delfino, F. Pampararo, M. Robba, and M. Rossi, "A dynamic optimization-based architecture for polygeneration microgrids with tri-generation, renewables, storage systems and electrical vehicles," *Energy Convers. Manage.*, vol. 96, pp. 511–520, May 2015, doi: 10.1016/j.enconman.2015.03.013.

[18] X. Jiang, L. Zhao, Y. Cheng, S. Wei, and Y. Jin, "Optimal configuration of electric vehicles for charging stations under the fast power supplement mode," *J. Energy Storage*, vol. 45, Jan. 2022, Art. no. 103677, doi: 10.1016/j.est.2021.103677.

[19] M. Sagar Bhaskar, V. K. Ramachandaramurthy, S. Padmanaban, F. Blaabjerg, D. M. Ionel, M. Mitolo, and D. Almakhles, "Survey of DC–DC non-isolated topologies for unidirectional power flow in fuel cell vehicles," *IEEE Access*, vol. 8, pp. 178130–178166, 2020, doi: 10.1109/ACCESS.2020.3027041.

[20] S. S. Sayed and A. M. Massoud, "Review on state-of-the-art unidirectional non-isolated power factor correction converters for short-/long-distance electric vehicles," *IEEE Access*, vol. 10, pp. 11308–11340, 2022, doi: 10.1109/ACCESS.2022.3146410.

[21] M. Pahlevani and P. K. Jain, "Soft-switching power electronics technology for electric vehicles: A technology review," *IEEE J. Emerg. Sel. Topics Ind. Electron.*, vol. 1, no. 1, pp. 80–90, Jul. 2020, doi: 10.1109/jestie.2020.2999590.

[22] S. LaMonaca and L. Ryan, "The state of play in electric vehicle charging services—A review of infrastructure provision, players, and policies," *Renew. Sustain. Energy Rev.*, vol. 154, Feb. 2022, Art. no. 111733, doi: 10.1016/j.rser.2021.111733.

[23] C. Will and A. Schuller, "Understanding user acceptance factors of electric vehicle smart charging," *Transp. Res. C, Emerg. Technol.*, vol. 71, pp. 198–214, Oct. 2016, doi: 10.1016/j.trc.2016.07.006.

[24] *Electric Vehicle Charging Definitions and Explanation*. Accessed: Jan. 2019. [Online]. Available: https://www.nklnederland.nl

[25] O. Sadeghian, A. Oshnoei, B. Mohammadi-ivatloo, V. Vahidinasab, and A. Anvari-Moghaddam, "A comprehensive review on electric vehicles smart charging: Solutions, strategies, technologies, and challenges," *J. Energy Storage*, vol. 54, Oct. 2022, Art. no. 105241, doi: 10.1016/j.est.2022.105241.

[26] A. Tomaszewska, Z. Chu, X. Feng, S. O'Kane, X. Liu, J. Chen, C. Ji, E. Endler, R. Li, L. Liu, Y. Li, S. Zheng, S. Vetterlein, M. Gao, J. Du, M. Parkes, M. Ouyang, M. Marinescu, G. Offer, and B. Wu, "Lithium-ion battery fast charging: A review," *eTransportation*, vol. 1, Aug. 2019, Art. no. 100011, doi: 10.1016/j.etran.2019.100011.

[27] M. Brenna, F. Foiadelli, C. Leone, and M. Longo, "Electric vehicles charging technology review and optimal size estimation," *J. Electr. Eng. Technol.*, vol. 15, no. 6, pp. 2539–2552, Nov. 2020, doi: 10.1007/s42835-020-00547-x.

[28] *Electric Car Sales Speed to 25,000 Units in April-November, Headed for 40,000 in FY2023 | Autocar Professional*. Accessed: Jan. 25, 2023. [Online]. Available: https://www.autocarpro.in/analysis-sales/electric-car-sales-speed-to-25000-units-in-april-november-headed-for-40000-in-fy2023-113606

[29] *EV Sales in India in 2022 record 210% Growth, Cross a Million for the First Time | Autocar Professional*. Accessed: Jan. 25, 2023. [Online]. Available: https://www.autocarpro.in/analysis-sales/ev-sales-in-india-in-2022-record-210-growth-cross-a-million-for-the-first-time-113710

[30] N. Kumar, T. Kumar, S. Nema, and T. Thakur, "A comprehensive planning framework for electric vehicles fast charging station assisted by solar and battery based on queueing theory and non-dominated sorting genetic algorithm-II in a co-ordinated transportation and power network," *J. Energy Storage*, vol. 49, May 2022, Art. no. 104180, doi: 10.1016/j.est.2022.104180.

[31] J. Wang, B. Wang, L. Zhang, J. Wang, N. I. Shchurov, and B. V. Malozyomov, "Review of bidirectional DC–DC converter topologies for hybrid energy storage system of new energy vehicles," *Green Energy Intell. Transp.*, vol. 1, no. 2, Sep. 2022, Art. no. 100010, doi: 10.1016/j.geits.2022.100010.

[32] S. D. Gore, A. Iqbal, S. Islam, I. Khan, M. Marzband, S. Rahman, and A. M. A. B. Al-Wahedi, "Review on classification of resonant converters for electric vehicle application," *Energy Rep.*, vol. 8, pp. 1091–1113, Nov. 2022, doi: 10.1016/j.egyr.2021.12.013.

[33] A. Kolli, A. Gaillard, A. De Bernardinis, O. Bethoux, D. Hissel, and Z. Khatir, "A review on DC/DC converter architectures for power fuel cell applications," *Energy Convers. Manage.*, vol. 105, pp. 716–730, Nov. 2015, doi: 10.1016/j.enconman.2015.07.060.

[34] *Vehicle Technologies Program—Multi-Year Program Plan 2011–2015*, Energy Efficiency Renew. Energy, USA, 2011.

[35] H. Tu, H. Feng, S. Srdic, and S. Lukic, "Extreme fast charging of electric vehicles: A technology overview," *IEEE Trans. Transport. Electrific.*, vol. 5, no. 4, pp. 861–878, Dec. 2019, doi: 10.1109/TTE.2019.2958709.

[36] G. Alkawsi, Y. Baashar, D. Abbas U, A. A. Alkahtani, and S. K. Tiong, "Review of renewable energy-based charging infrastructure for electric vehicles," *Appl. Sci.*, vol. 11, no. 9, p. 3847, Apr. 2021, doi: 10.3390/app11093847.

[37] K. Sayed, A. Almutairi, N. Albagami, O. Alrumayh, A. G. Abo-Khalil, and H. Saleeb, "A review of DC-AC converters for electric vehicle applications," *Energies*, vol. 15, no. 3, p. 1241, Feb. 2022, doi: 10.3390/en15031241.

[38] X. Duan, Z. Hu, Y. Song, K. Strunz, Y. Cui, and L. Liu, "Planning strategy for an electric vehicle fast charging service provider in a competitive environment," *IEEE Trans. Transport. Electrific.*, vol. 8, no. 3, pp. 3056–3067, Sep. 2022, doi: 10.1109/TTE.2022.3152387.

[39] Q. Cheng, L. Chen, Q. Sun, R. Wang, D. Ma, and D. Qin, "A smart charging algorithm based on a fast charging station without energy storage system," *CSEE J. Power Energy Syst.*, vol. 7, no. 4, pp. 850–861, Jul. 2021, doi: 10.17775/CSEEJPES.2020.00350.

[40] N. Mohamed, F. Aymen, T. E. A. Alharbi, C. Z. El-Bayeh, S. Lassaad, S. S. M. Ghoneim, and U. Eicker, "A comprehensive analysis of wireless charging systems for electric vehicles," *IEEE Access*, vol. 10, pp. 43865–43881, 2022, doi: 10.1109/ACCESS.2022.3168727.

[41] F. Grazian, T. B. Soeiro, and P. Bauer, "Voltage/current doubler converter for an efficient wireless charging of electric vehicles with 400-V and 800-V battery voltages," *IEEE Trans. Ind. Electron.*, vol. 70, no. 8, pp. 7891–7903, Aug. 2023, doi: 10.1109/TIE.2022.3208582.

[42] Z. Zhou, L. Zhang, Z. Liu, Q. Chen, R. Long, and H. Su, "Model predictive control for the receiving-side DC–DC converter of dynamic wireless power transfer," *IEEE Trans. Power Electron.*, vol. 35, no. 9, pp. 8985–8997, Sep. 2020, doi: 10.1109/TPEL.2020.2969996.

[43] Y. Zhang, Y. Wu, Z. Shen, W. Pan, H. Wang, J. Dong, X. Mao, and X. Liu, "Integration of onboard charger and wireless charging system for electric vehicles with shared coupler, compensation, and rectifier," *IEEE Trans. Ind. Electron.*, vol. 70, no. 7, pp. 7511–7514, Jul. 2023, doi: 10.1109/TIE.2022.3204857.

[44] S. A. Gorji, H. G. Sahebi, M. Ektesabi, and A. B. Rad, "Topologies and control schemes of bidirectional DC–DC power converters: An overview," *IEEE Access*, vol. 7, pp. 117997–118019, 2019, doi: 10.1109/ACCESS.2019.2937239.

[45] A. Govind, R. A. Rajitha, and S. Rajalakshmy, "A review of high-gain bidirectional DC–DC converter with reduced ripple current," in *Proc. 3rd Int. Conf. Intell. Comput. Instrum. Control Technol. (ICICICT)*, Aug. 2022, pp. 211–216, doi: 10.1109/ICICICT54557.2022.9917677.

[46] Y. Guan, C. Cecati, J. M. Alonso, and Z. Zhang, "Review of high-frequency high-voltage-conversion-ratio DC–DC converters," *IEEE J. Emerg. Sel. Topics Ind. Electron.*, vol. 2, no. 4, pp. 374–389, Oct. 2021, doi: 10.1109/jestie.2021.3051554.

[47] D. Savio Abraham, R. Verma, L. Kanagaraj, S. R. Giri Thulasi Raman, N. Rajamanickam, B. Chokkalingam, K. Marimuthu Sekar, and L. Mihet-Popa, "Electric vehicles charging Stations' architectures, criteria, power converters, and control strategies in microgrids," *Electronics*, vol. 10, no. 16, p. 1895, Aug. 2021, doi: 10.3390/electronics10161895.

[48] S. S. Sayed and A. M. Massoud, "Review on state-of-the-art unidirectional non-isolated power factor correction converters for short-/long-distance electric vehicles," *IEEE Access*, vol. 10, pp. 11308–11340, 2022, doi: 10.1109/ACCESS.2022.3146410.

[49] S. Vijayakumar and N. Sudhakar, "A review on unidirectional converters for on-board chargers in electric vehicle," *Frontiers Energy Res.*, vol. 10, Oct. 2022, Art. no. 1011681, doi: 10.3389/fenrg.2022.1011681.

[50] F. N. Esfahani, A. Darwish, and B. W. Williams, "Power converter topologies for grid-tied solar photovoltaic (PV) powered electric vehicles (EVs)—A comprehensive review," *Energies*, vol. 15, no. 13, p. 4648, Jun. 2022, doi: 10.3390/en15134648.

[51] I. Jagadeesh and V. Indragandhi, "Review and comparative analysis on DC–DC converters used in electric vehicle applications," *IOP Conf. Mater. Sci. Eng.*, vol. 623, Oct. 2019, Art. no. 012005, doi: 10.1088/1757-899X/623/1/012005.

[52] R. Fachrizal, M. Shepero, D. van der Meer, J. Munkhammar, and J. Widén, "Smart charging of electric vehicles considering photovoltaic power production and electricity consumption: A review," *eTransportation*, vol. 4, May 2020, Art. no. 100056, doi: 10.1016/j.etran.2020.100056.

[53] G. Rituraj, G. R. C. Mouli, and P. Bauer, "A comprehensive review on off-grid and hybrid charging systems for electric vehicles," *IEEE Open J. Ind. Electron. Soc.*, vol. 3, pp. 203–222, 2022, doi: 10.1109/OJIES.2022.3167948.

[54] A. Khaligh and M. D'Antonio, "Global trends in high-power on-board chargers for electric vehicles," *IEEE Trans. Veh. Technol.*, vol. 68, no. 4, pp. 3306–3324, Apr. 2019.

[55] C. Balaji, C. Anuradha, N. Chellammal, and R. Bharadwaj, "An extendable high-efficiency triple-port SEPIC–SEPIC converter with continuous input currents for DC microgrid applications," *Int. Trans. Electr. Energy Syst.*, vol. 31, no. 11, p. e1312, Nov. 2021, doi: 10.1002/2050-7038.13121.

[56] B. Chandrasekar, C. Nallaperumal, S. Padmanaban, M. S. Bhaskar, J. B. Holm-Nielsen, Z. Leonowicz, and S. O. Masebinu, "Non-isolated high-gain triple port DC–DC buck-boost converter with positive output voltage for photovoltaic applications," *IEEE Access*, vol. 8, pp. 113649–113666, 2020, doi: 10.1109/ACCESS.2020.3003192.

[57] (2016). *Electric Vehicles Infrastructure for Fleet Operations IET Standards Technical Briefi Ng*. [Online]. Available: https://www.theiet.org

[58] I. Aretxabaleta, I. M. De Alegria, J. Andreu, I. Kortabarria, and E. Robles, "High-voltage stations for electric vehicle fast-charging: Trends, standards, charging modes and comparison of unity power-factor rectifiers," *IEEE Access*, vol. 9, pp. 102177–102194, 2021, doi: 10.1109/ACCESS.2021.3093696.

[59] B. Chandrasekar, N. Chellammal, and B. Nallamothu, "Non-isolated unidirectional three-port Cuk-Cuk converter for fuel cell/solar Pv systems," *J. Power Electron.*, vol. 19, no. 5, pp. 1278–1288, Sep. 2019, doi: 10.6113/JPE.2019.19.5.1278.

[60] M. R. Khalid, I. A. Khan, S. Hameed, M. S. J. Asghar, and J.-S. Ro, "A comprehensive review on structural topologies, power levels, energy storage systems, and standards for electric vehicle charging stations and their impacts on grid," *IEEE Access*, vol. 9, pp. 128069–128094, 2021, doi: 10.1109/ACCESS.2021.3112189.

[61] R. Rahimi, S. Habibi, M. Ferdowsi, and P. Shamsi, "Z-source-based high step-up DC–DC converters for photovoltaic applications," *IEEE J. Emerg. Sel. Topics Power Electron.*, vol. 10, no. 4, pp. 4783–4796, Aug. 2022, doi: 10.1109/JESTPE.2021.3131996.

[62] S. Habib, M. M. Khan, F. Abbas, A. Ali, M. T. Faiz, F. Ehsan, and H. Tang, "Contemporary trends in power electronics converters for charging solutions of electric vehicles," *CSEE J. Power Energy Syst.*, vol. 6, no. 4, pp. 911–929, Dec. 2020, doi: 10.17775/CSEEJPES.2019.02700.

[63] B. Chandrasekar, C. Nallaperumal, and S. Dash, "A nonisolated three-port DC–DC converter with continuous input and output currents based on cuk topology for PV/Fuel cell applications," *Electronics*, vol. 8, no. 2, p. 214, Feb. 2019, doi: 10.3390/electronics8020214.

[64] A. Joseph, S. S, and A. M. George, "A review of DC DC converters for renewable energy and EV charging applications," in *Proc. 3rd Int. Conf. Intell. Comput. Instrum. Control Technol. (ICICICT)*, Aug. 2022, pp. 245–250, doi: 10.1109/ICICICT54557.2022.9917935.

[65] L. Schmitz, D. C. Martins, and R. F. Coelho, "Conception of high step-up DC–DC boost-based converters," in *Proc. Brazilian Power Electron. Conf. (COBEP)*, Nov. 2017, pp. 1–6, doi: 10.1109/COBEP.2017.8257241.

[66] L. Schmitz, D. C. Martins, and R. F. Coelho, "Generalized high step-up DC–DC boost-based converter with gain cell," *IEEE Trans. Circuits Syst. I, Reg. Papers*, vol. 64, no. 2, pp. 480–493, Feb. 2017, doi: 10.1109/TCSI.2016.2603782.

[67] V. F. Pires, A. Cordeiro, D. Foito, and J. F. Silva, "High step-up DC–DC converter for fuel cell vehicles based on merged quadratic Boost–Cuk," *IEEE Trans. Veh. Technol.*, vol. 68, no. 8, pp. 7521–7530, Aug. 2019, doi: 10.1109/TVT.2019.2921851.

[68] K. Zaoskoufis and E. C. Tatakis, "An improved boost-based DC/DC converter with high-voltage step-up ratio for DC microgrids," *IEEE J. Emerg. Sel. Topics Power Electron.*, vol. 9, no. 2, pp. 1837–1853, Apr. 2021, doi: 10.1109/JESTPE.2020.2981018.

[69] B. Forouzesh, M. Siwakoti, P. Yam Gorji, A. S. Blaabjerg, and F. Lehman, "Step-up DC–DC Converters: A comprehensive review of voltage-boosting techniques, topologies, and applications," *IEEE Trans. Power Electron.*, vol. 32, pp. 9143–9178, 2017.

[70] D. Gautam, A. K. Sharma, and J. Shukla, "A review of voltage boosting techniques for step-up DC–DC converter," *IJIREEICE*, vol. 7, no. 6, pp. 35–41, Jun. 2019, doi: 10.17148/ijireeice.2019.7607.

[71] N. Korada and R. Ayyanar, "Novel quadratic high gain boost converter with adaptive soft-switching scheme and reduced conduction loss," *IEEE Trans. Ind. Appl.*, vol. 58, no. 6, pp. 7421–7431, Nov. 2022, doi: 10.1109/TIA.2022.3193880.

[72] M. Ashok Bhupathi Kumar and V. Krishnasamy, "Quadratic boost converter with less input current ripple and rear-end capacitor voltage stress for renewable energy applications," *IEEE J. Emerg. Sel. Topics Power Electron.*, vol. 10, no. 2, pp. 2265–2275, Apr. 2022, doi: 10.1109/JESTPE.2021.3122354.

[73] X. Liu, X. Zhang, X. Hu, H. Chen, L. Chen, and Y. Zhang, "Interleaved high step-up converter with coupled inductor and voltage multiplier for renewable energy system," *CPSS Trans. Power Electron. Appl.*, vol. 4, no. 4, pp. 299–309, Dec. 2019, doi: 10.24295/CPSSTPEA.2019.00028.

[74] R. R. Khorasani, H. M. Jazi, N. R. Chaudhuri, A. Khoshkbar-Sadigh, M. Shaneh, E. Adib, and P. Wheeler, "An interleaved soft switched high step-up boost converter with high power density for renewable energy applications," *IEEE Trans. Power Electron.*, vol. 37, no. 11, pp. 13782–13798, Nov. 2022, doi: 10.1109/TPEL.2022.3181946.

[75] P. Mohseni, S. Mohammadsalehian, Md. R. Islam, K. M. Muttaqi, D. Sutanto, and P. Alavi, "Ultrahigh voltage gain DC–DC boost converter with ZVS switching realization and coupled inductor extendable voltage multiplier cell techniques," *IEEE Trans. Ind. Electron.*, vol. 69, no. 1, pp. 323–335, Jan. 2022, doi: 10.1109/TIE.2021.3050385.

[76] B. Yuan, L. Liao, G. Ning, W. Xiong, and M. Su, "An expandable high voltage-gain resonant DC–DC converter with low semiconductor voltage stress," *IEEE Trans. Circuits Syst. II, Exp. Briefs*, vol. 69, no. 9, pp. 3844–3848, Sep. 2022, doi: 10.1109/TCSII.2022.3175825.

[77] A. Pandey and S. Pattnaik, "Design and analysis of extendable switched-inductor and capacitor-divider network based high-boost DC–DC converter for solar PV application," *IEEE Access*, vol. 10, pp. 66992–67007, 2022, doi: 10.1109/ACCESS.2022.3185107.

[78] P. E. Babu, S. Vemparala, T. Pavithra, and S. Kumaravel, "Switched LC network-based multistage ultra gain DC–DC converter," *IEEE Access*, vol. 10, pp. 64701–64714, 2022, doi: 10.1109/ACCESS.2022.3183015.

[79] N. A. Ahmed, B. N. Alajmi, I. Abdelsalam, and M. I. Marei, "Soft switching multiphase interleaved boost converter with high voltage gain for EV applications," *IEEE Access*, vol. 10, pp. 27698–27716, 2022, doi: 10.1109/ACCESS.2022.3157050.

[80] S. Sadaf, M. S. Bhaskar, M. Meraj, A. Iqbal, and N. Al-Emadi, "Transformer-less boost converter with reduced voltage stress for high voltage step-up applications," *IEEE Trans. Ind. Electron.*, vol. 69, no. 2, pp. 1498–1508, Feb. 2022, doi: 10.1109/TIE.2021.3055166.

[81] M. Veerachary and P. Sen, "Dual-switch enhanced gain boost DC–DC converters," *IEEE Trans. Ind. Appl.*, vol. 58, no. 4, pp. 4903–4913, Jul. 2022, doi: 10.1109/TIA.2022.3171533.

[82] R. Stala, Z. Waradzyn, and S. Folmer, "Input current ripple reduction in a step-up DC–DC switched-capacitor switched-inductor converter," *IEEE Access*, vol. 10, pp. 19890–19904, 2022, doi: 10.1109/ACCESS.2022.3152543.

[83] S. Pirpoor, S. Rahimpour, M. Andi, N. Kanagaraj, S. Pirouzi, and A. H. Mohammed, "A novel and high-gain switched-capacitor and switched-inductor-based DC/DC boost converter with low input current ripple and mitigated voltage stresses," *IEEE Access*, vol. 10, pp. 32782–32802, 2022, doi: 10.1109/ACCESS.2022.3161576.

[84] K. Bekkam and V. Karthikeyan, "Ultra-voltage gain step-up DC–DC converter for renewable energy micro-source applications," *IEEE Trans. Energy Convers.*, vol. 37, no. 2, pp. 947–957, Jun. 2022, doi: 10.1109/TEC.2021.3116076.

[85] S. Kumaravel and P. E. Babu, "Reduced switch voltage stress ultra-gain DC–DC converter for high voltage low power applications," *IEEE Trans. Circuits Syst. II, Exp. Briefs*, vol. 69, no. 3, pp. 1277–1281, Mar. 2022, doi: 10.1109/TCSII.2021.3107552.

[86] X. Ding, M. Zhou, Y. Cao, B. Li, Y. Sun, and X. Hu, "A high step-up coupled-inductor-integrated DC–DC multilevel boost converter with continuous input current," *IEEE J. Emerg. Sel. Topics Power Electron.*, vol. 10, no. 6, pp. 7346–7360, Dec. 2022, doi: 10.1109/JESTPE.2022.3184699.

[87] V. Abbasi, S. Rostami, S. Hemmati, and S. Ahmadian, "Ultrahigh step-up quadratic boost converter using coupled inductors with low voltage stress on the switches," *IEEE J. Emerg. Sel. Topics Power Electron.*, vol. 10, no. 6, pp. 7733–7743, Dec. 2022, doi: 10.1109/JESTPE.2022.3195817.

[88] C. L. Narayana, H. M. Suryawanshi, P. Nachankar, P. Vijaya Vardhan Reddy, and D. Govind, "A quintupler boost high conversion gain soft-switched converter for DC microgrid," *IEEE Trans. Circuits Syst. II, Exp. Briefs*, vol. 69, no. 3, pp. 1287–1291, Mar. 2022, doi: 10.1109/TCSII.2021.3105638.

[89] S. Gao, X. Sang, Y. Wang, Y. Liu, Y. Guan, and D. Xu, "A DCM high-frequency high-step-up SEPIC-based converter with extended ZVS range," *IEEE J. Emerg. Sel. Topics Power Electron.*, vol. 10, no. 6, pp. 7915–7924, Dec. 2022, doi: 10.1109/JESTPE.2021.3051168.

[90] S. A. Ansari and J. S. Moghani, "A novel high voltage gain noncoupled inductor SEPIC converter," *IEEE Trans. Ind. Electron.*, vol. 66, no. 9, pp. 7099–7108, Sep. 2019, doi: 10.1109/TIE.2018.2878127.

[91] S. Gao, Y. Wang, Y. Guan, and D. Xu, "A high step up SEPIC-based converter based on partly interleaved transformer," *IEEE Trans. Ind. Electron.*, vol. 67, no. 2, pp. 1455–1465, Feb. 2020, doi: 10.1109/TIE.2019.2910044.

[92] S. Gao, Y. Wang, Y. Liu, Y. Guan, and D. Xu, "A novel DCM soft-switched SEPIC-based high-frequency converter with high step-up capacity," *IEEE Trans. Power Electron.*, vol. 35, no. 10, pp. 10444–10454, Oct. 2020, doi: 10.1109/TPEL.2020.2975130.

[93] A. Mostaan, J. Yuan, Y. P. Siwakoti, S. Esmaeili, and F. Blaabjerg, "A trans-inverse coupled-inductor semi-SEPIC DC/DC converter with full control range," *IEEE Trans. Power Electron.*, vol. 34, no. 11, pp. 10398–10402, Nov. 2019, doi: 10.1109/TPEL.2019.2917306.

[94] Y. P. Siwakoti, A. Mostaan, A. Abdelhakim, P. Davari, M. N. Soltani, Md. N. H. Khan, L. Li, and F. Blaabjerg, "High-voltage gain quasi-SEPIC DC–DC converter," *IEEE J. Emerg. Sel. Topics Power Electron.*, vol. 7, no. 2, pp. 1243–1257, Jun. 2019, doi: 10.1109/JESTPE.2018.2859425.

[95] S.-W. Lee and H.-L. Do, "Isolated SEPIC DC–DC converter with ripple-free input current and lossless snubber," *IEEE Trans. Ind. Electron.*, vol. 65, no. 2, pp. 1254–1262, Feb. 2018, doi: 10.1109/TIE.2017.2733440.

[96] M. R. Banaei and S. G. Sani, "Analysis and implementation of a new SEPIC-based single-switch buck–boost DC–DC converter with continuous input current," *IEEE Trans. Power Electron.*, vol. 33, no. 12, pp. 10317–10325, Dec. 2018, doi: 10.1109/TPEL.2018.2799876.

[97] P. J. S. Costa, C. H. Illa Font, and T. B. Lazzarin, "Single-phase hybrid switched-capacitor voltage-doubler SEPIC PFC rectifiers," *IEEE Trans. Power Electron.*, vol. 33, no. 6, pp. 5118–5130, Jun. 2018, doi: 10.1109/TPEL.2017.2737534.

[98] S. Gao, Y. Wang, Y. Guan, and D. Xu, "A high-frequency high voltage gain modified SEPIC with integrated inductors," *IEEE Trans. Ind. Appl.*, vol. 55, no. 6, pp. 7481–7490, Nov. 2019, doi: 10.1109/TIA.2019.2909498.

[99] B. Andres, L. Romitti, A. M. S. S. Andrade, L. Roggia, and L. Schuch, "Comprehensive analysis of voltage step-up techniques for isolated SEPIC," *IEEE Trans. Circuits Syst. I, Reg. Papers*, vol. 69, no. 10, pp. 4298–4311, Oct. 2022, doi: 10.1109/TCSI.2022.3189884.

[100] S. Hasanpour, M. Forouzesh, Y. P. Siwakoti, and F. Blaabjerg, "A new high-gain, high-efficiency SEPIC-based DC–DC converter for renewable energy applications," *IEEE J. Emerg. Sel. Topics Ind. Electron.*, vol. 2, no. 4, pp. 567–578, Oct. 2021, doi: 10.1109/jestie.2021.3074864.

[101] P. K. Maroti, S. Padmanaban, J. B. Holm-Nielsen, M. S. Bhaskar, M. Meraj, and A. Iqbal, "A new structure of high voltage gain SEPIC converter for renewable energy applications," *IEEE Access*, vol. 7, pp. 89857–89868, 2019, doi: 10.1109/ACCESS.2019.2925564.

[102] H. Ardi and A. Ajami, "Study on a high voltage gain SEPIC-based DC–DC converter with continuous input current for sustainable energy applications," *IEEE Trans. Power Electron.*, vol. 33, no. 12, pp. 10403–10409, Dec. 2018, doi: 10.1109/TPEL.2018.2811123.

[103] P. J. S. Costa, M. V. M. Ewerling, C. H. I. Font, and T. B. Lazzarin, "Unidirectional three-phase voltage-doubler SEPIC PFC rectifier," *IEEE Trans. Power Electron.*, vol. 36, no. 6, pp. 6761–6773, Jun. 2021, doi: 10.1109/TPEL.2020.3037480.

[104] S. Hasanpour, T. Nouri, F. Blaabjerg, and Y. P. Siwakoti, "High step-up SEPIC-based trans-inverse DC–DC converter with quasi-resonance operation for renewable energy applications," *IEEE Trans. Ind. Electron.*, vol. 70, no. 1, pp. 485–497, Jan. 2023, doi: 10.1109/TIE.2022.3150103.

[105] F. I. Kravetz and R. Gules, "Soft-switching high static gain modified SEPIC converter," *IEEE J. Emerg. Sel. Topics Power Electron.*, vol. 9, no. 6, pp. 6739–6747, Dec. 2021, doi: 10.1109/JESTPE.2021.3079573.

[106] S. Hasanpour, A. Baghramian, and H. Mojallali, "A modified SEPIC-based high step-up DC–DC converter with quasi-resonant operation for renewable energy applications," *IEEE Trans. Ind. Electron.*, vol. 66, no. 5, pp. 3539–3549, May 2019, doi: 10.1109/TIE.2018.2851952.

[107] S. Mahdizadeh, H. Gholizadeh, and S. A. Gorji, "A power converter based on the combination of cuk and positive output super lift lou converters: Circuit analysis, simulation and experimental validation," *IEEE Access*, vol. 10, pp. 52899–52911, 2022, doi: 10.1109/ACCESS.2022.3175892.

[108] A. M. S. S. Andrade, T. M. K. Faistel, A. Toebe, and R. A. Guisso, "Family of transformerless active switched inductor and switched capacitor ćuk DC–DC converter for high voltage gain applications," *IEEE J. Emerg. Sel. Topics Ind. Electron.*, vol. 2, no. 4, pp. 390–398, Oct. 2021, doi: 10.1109/jestie.2021.3091419.

[109] E. Sehirli, "Analysis of LCL filter topologies for DC–DC isolated cuk converter at CCM operation," *IEEE Access*, vol. 10, pp. 113741–113755, 2022, doi: 10.1109/access.2022.3218162.

[110] B. Zhu, G. Liu, Y. Zhang, Y. Huang, and S. Hu, "Single-switch high step-up zeta converter based on coat circuit," *IEEE Access*, vol. 9, pp. 5166–5176, 2021, doi: 10.1109/ACCESS.2020.3048388.

[111] B. Zhu, Y. Liu, S. Zhi, K. Wang, and J. Liu, "A family of bipolar high step-up zeta–buck–boost converter based on 'coat circuit," *IEEE Trans. Power Electron*, vol. 38, no. 3, pp. 3328–3339, Nov. 2022, doi: 10.1109/tpel.2022.3221781.

[112] M. S. Bhaskar, N. Gupta, S. Selvam, D. J. Almakhles, P. Sanjeevikumar, J. S. M. Ali, and S. Umashankar, "A new hybrid zeta-boost converter with active quad switched inductor for high voltage gain," *IEEE Access*, vol. 9, pp. 20022–20034, 2021, doi: 10.1109/ACCESS.2021.3054393.

[113] M. R. Banaei and H. A. F. Bonab, "A high efficiency nonisolated buck–boost converter based on ZETA converter," *IEEE Trans. Ind. Electron.*, vol. 67, no. 3, pp. 1991–1998, Mar. 2020, doi: 10.1109/TIE.2019.2902785.

[114] R. Kushwaha and B. Singh, "Bridgeless isolated Zeta–Luo converter-based EV charger with PF preregulation," *IEEE Trans. Ind. Appl.*, vol. 57, no. 1, pp. 628–636, Jan. 2021, doi: 10.1109/TIA.2020.3036019.

[115] R. S. Devi, P. V. Mrudhulaa, K. Priyadharshini, R. Seyezhai, and M. Vempati, "Development of solar DC home system using modified LUO converter," *Int J. Eng. Adv. Technol.*, vol. 8, no. 1, pp. 23–30, Oct. 2018.

[116] B. Faridpak, M. Farrokhifar, M. Nasiri, A. Alahyari, and N. Sadoogi, "Developing a super-lift luo-converter with integration of buck converters for electric vehicle applications," *CSEE J. Power Energy Syst.*, vol. 7, no. 4, pp. 811–820, Jul. 2021, doi: 10.17775/CSEEJPES.2020.01880.

[117] R. Kushwaha and B. Singh, "Design and development of modified BL luo converter for PQ improvement in EV charger," *IEEE Trans. Ind. Appl.*, vol. 56, no. 4, pp. 3976–3984, Jul. 2020, doi: 10.1109/TIA.2020.2988197.

[118] B. Singh and R. Kushwaha, "Power factor preregulation in interleaved luo converter-fed electric vehicle battery charger," *IEEE Trans. Ind. Appl.*, vol. 57, no. 3, pp. 2870–2882, May 2021, doi: 10.1109/TIA.2021.3061964.

[119] F. Ghasemi, M. R. Yazdani, and M. Delshad, "Step-up DC–DC switching converter with single switch and multi-outputs based on luo topology," *IEEE Access*, vol. 10, pp. 16871–16882, 2022, doi: 10.1109/ACCESS.2022.3150316.

[120] J. D. Navamani, A. Geetha, D. Almakhles, A. Lavanya, and J. S. M. Ali, "Modified LUO high gain DC–DC converter with minimal capacitor stress for electric vehicle application," *IEEE Access*, vol. 9, pp. 122335–122350, 2021, doi: 10.1109/ACCESS.2021.3109273.

[121] J. Gupta and B. Singh, "Bridgeless isolated positive output luo converter based high power factor single stage charging solution for light electric vehicles," *IEEE Trans. Ind. Appl.*, vol. 58, no. 1, pp. 732–741, Jan. 2022, doi: 10.1109/TIA.2021.3131647.

[122] J. Ai, M. Lin, H. Liu, and P. Wheeler, "A family of high step–up DC–DC converters with nc step-up cells and M–source clamped circuits," *IEEE Access*, vol. 9, pp. 65947–65966, 2021, doi: 10.1109/ACCESS.2021.3073416.

R. VENUGOPAL received the B.E. degree in electrical and electronic engineering and the M.E. degree in power electronics and drives from the Jerusalem College of Engineering, affiliated to Anna University, Chennai, in 2009 and 2011, respectively. He is currently pursuing the Ph.D. degree in electrical and electronic engineering with the SRM Institute of Science and Technology, Kattankulathur, Chennai, Tamil Nadu, India.

From 2011 to 2012, he was an Assistant Professor with the Sri Lakshmi Ammal Engineering College, Chennai. From 2012 to 2014, he was associated with the Dhanalakshmi College of Engineering, Chennai, as an Assistant Professor. From 2014 to 2017, he was an Assistant Professor with the Kingston Engineering College, Vellore, and from 2017 to 2021, he was with the Saranathan College of Engineering as an Assistant Professor.

Mr. Venugopal was a Life Member of Indian Society for Technical Education (ISTE), Institution of Engineering and Technology (IET), and International Association of Engineers (INEAG).

BALAJI CHANDRASEKAR (Member, IEEE) was born in Arakkonam, India. He received the B.E. degree in electrical and electronics engineering from the IFET College of Engineering, Villupuram, and the M.E. degree in control and instrumentation engineering from the College of Engineering, Guindy, Anna University, India. He completed his research in the area of power electronics from the Department of Electrical and Electronics Engineering, SRM Institute of Science and Technology (SRMIST), Kattankulathur, Chennai. He is currently an Assistant Professor with the Department of Electrical and Electronics Engineering, SRMIST. He has authored more than 17 technical papers published in journals and conference proceedings. He has also authored a book titled *Measurement and Instrumentation* for undergraduate students. His current research interests include multi-port power electronic converters and renewable energy systems. He is a member of the Institution of Engineers, India, and Indian Society for Technical Education, India.

A. DOMINIC SAVIO (Member, IEEE) received the B.E. degree in electrical engineering from Anna University, in 2007, the M.Tech. degree in control and instrumentation from Karunya University, Coimbatore, in 2010, and the Ph.D. degree from the SRM Institute of Science and Technology (SRMIST), India, in 2020. He is currently an Assistant Professor with the Department of Electrical and Electronics Engineering, SRMIST. He has authored more than 17 technical papers published in journals and conference proceedings. His research interests include power management and control in electric vehicle charging infrastructure and electric vehicle charging converter. He is a member of the Institution of Engineers, India.

R. NARAYANAMOORTHI (Member, IEEE) received the bachelor's degree in electrical engineering and the master's degree in control and instrumentation from Anna University, India, in 2009 and 2011, respectively, and the Ph.D. degree from the SRM Institute of Science and Technology (SRMIST), India, in 2019. He is currently an Associate Professor with the Department of Electrical and Electronics Engineering, SRMIST. His research interests include wireless power transfer, electric vehicles, power electronics, artificial intelligence and machine learning in renewable energy systems, and embedded systems for smart sensors.

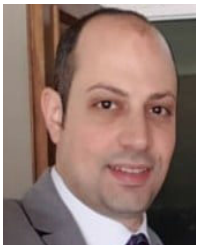

KAREEM M. ABORAS received the B.Sc., M.Sc., and Ph.D. degrees in electrical engineering from the Faculty of Engineering, Alexandria University, Alexandria, Egypt, in 2010, 2015, and 2020, respectively. His Ph.D. research work is focused on the performance enhancement of renewable energy conversion systems. Currently, he is an Assistant Professor with the Electrical Power and Machines Department, Faculty of Engineering, Alexandria University. His research interests include power electronics, control, drives, power systems, and renewable energy systems. He is a reviewer of IET journal.

HOSSAM KOTB received the B.Sc., M.Sc., and Ph.D. degrees in electrical engineering from the Faculty of Engineering, Alexandria University, Alexandria, Egypt, in 2009, 2013, and 2020, respectively. His Ph.D. research work is focused on the performance enhancement of renewable energy conversion systems. Currently, he is an Assistant Professor with the Electrical Power and Machines Department, Faculty of Engineering, Alexandria University. His research interests include power system analysis, electrical drives, modern control techniques, smart grids, optimization, electric vehicles, and renewable energy systems. He is also an Associate Editor of *Alexandria Engineering Journal* (AEJ).

YAZEED YASIN GHADI received the Ph.D. degree in electrical and computer engineering from The University of Queensland. He was a Postdoctoral Researcher with The University of Queensland, before joining Al Ain University. He is currently an Assistant Professor in software engineering with Al Ain University. He has published more than 25 peer-reviewed journals and conference papers and he holds three pending patents. His current research interests include developing novel electro-acoustic-optic neural interfaces for large-scale high-resolution electrophysiology and distributed optogenetic stimulation. He was a recipient of several awards. His dissertation on developing novel hybrid plasmonic photonic on-chip biochemical sensors received the Sigma Xi Best Ph.D. Thesis Award.

MOKHTAR SHOURAN received the B.Sc. and M.Sc. degrees in control engineering from the College of Electronics Technology, Bani Waled, Libya, in 2011 and 2014, respectively, the M.Sc. degree in electronics and information technology from the University of South Wales, Treforest, U.K., in 2017, and the Ph.D. degree in power systems stability and control from the School of Engineering, Cardiff University, Cardiff, U.K., in 2023. His research interests include optimization algorithms, fuzzy logic control, sliding mode control, traditional control, power system stability, and robotics. He was also awarded a certificate of excellence in electronics and information technology from the University of South Wales.

ELMAZEG ELGAMLI received the H.D. degree in electrical and electronics engineering from the College of Science and Technology—Qaminis, Libya, in 2009, and the M.Sc. degree in electronics and information technology in U.K., in 2017. He is currently pursuing the Ph.D. degree with the School of Engineering, Cardiff University, U.K. His research interests include magnetic materials and magnetic material and characterization magnetic materials.